REGULAR ARTICLE

blood advances

Not just a marker: CD34 on human hematopoietic stem/progenitor cells dominates vascular selectin binding along with CD44

Dina B. AbuSamra,[1] Fajr A. Aleisa,[1] Asma S. Al-Amoodi,[1] Heba M. Jalal Ahmed,[1] Chee Jia Chin,[1] Ayman F. Abuelela,[1] Ptissam Bergam,[2] Rachid Sougrat,[2] and Jasmeen S. Merzaban[1]

[1]Cell Migration and Signaling Laboratory, Division of Biological and Environmental Sciences and Engineering, and [2]Imaging and Characterization Core Facility, King Abdullah University of Science and Technology, Thuwal, Saudi Arabia

Key Points

- Human HSPCs expressing CD34 exhibit E-selectin binding activity, whereas those lacking CD34 do not.
- CD34 is a unique E- and P-selectin ligand on human HSPCs that binds with kinetics comparable to other known selectin ligands.

CD34 is routinely used to identify and isolate human hematopoietic stem/progenitor cells (HSPCs) for use clinically in bone marrow transplantation, but its function on these cells remains elusive. Glycoprotein ligands on HSPCs help guide their migration to specialized microvascular beds in the bone marrow that express vascular selectins (E- and P-selectin). Here, we show that HSPC-enriched fractions from human hematopoietic tissue expressing CD34 ($CD34^{pos}$) bound selectins, whereas those lacking CD34 ($CD34^{neg}$) did not. An unbiased proteomics screen identified potential glycoprotein ligands on $CD34^{pos}$ cells revealing CD34 itself as a major vascular selectin ligand. Biochemical and CD34 knockdown analyses highlight a key role for CD34 in the first prerequisite step of cell migration, suggesting that it is not just a marker on these cells. Our results also entice future potential strategies to investigate the glycoforms of CD34 that discriminate normal HSPCs from leukemic cells and to manipulate $CD34^{neg}$ HSPC-enriched bone marrow or cord blood populations as a source of stem cells for clinical use.

Introduction

Hematopoietic stem cells (HSCs) are rare cells that are maintained throughout life (self-renewing). They produce hematopoietic progenitor cells that differentiate into every type of mature blood cell within a well-defined hierarchy. Among hematopoietic stem/progenitor cell (HSPC) markers, CD34 is well known for its unique expression on HSPCs. For this reason, it is used to enrich donor bone marrow (BM) with HSPCs prior to BM transplantation.[1] Although the role of CD34 as a marker of HSCs is under debate,[2,3] recent studies suggest the existence of a population of dormant human HSCs that are CD34 negative ($CD34^{neg}$) but become positive ($CD34^{pos}$) just prior to cell division.[4-8] Studying this negative population is challenging because a defined marker for its enrichment is still lacking and also because it demonstrates extremely poor homing and engraftment capabilities compared with its $CD34^{pos}$ counterpart.[9-11] Studies of gene expression comparing lineage negative fractions of human peripheral blood HSPCs that either express the CD34 antigen or not imply that $CD34^{neg}$ HSPC subsets are more kinetically and functionally dormant, whereas CD34 expression in $CD34^{pos}$ HSPCs is related to cell cycle entry, metabolic activation, and HSPC mobilization and homing.[12-15] However, a detailed explanation of how CD34 contributes to $CD34^{pos}$ HSPC engraftment into the BM remains unknown.

To date, the functional role of CD34 in migration has most clearly been understood in the context of recruitment of lymphocytes to specialized high endothelial venules[16-18] that line the secondary lymphoid organs. Naive T cells home to these lymphoid organs in a multistep process that involves initial tethering and rolling interactions with CD34 (along with other ligands with restricted expression to high endothelial venules, often referred to as peripheral node addressins) mediated by the L-selectin expressed on the migrating T cells.[16,17] In fact, ectopic expression of CD34 in murine T cells promoted

Submitted 2 May 2017; accepted 10 November 2017. DOI 10.1182/bloodadvances.2017004317.

The full-text version of this article contains a data supplement.

their binding to human (but not mouse) BM stromal cells, suggesting that CD34 may bind a counterreceptor expressed on human BM endothelial cells to promote their homing.[10] In support of this hypothesis, studies using CD34 knockout mice indicate that CD34 increases trafficking and migration of hematopoietic cells[11,19]; however, the precise mechanism is still not fully understood.

Studies in both humans and mice indicate that E-selectin and P-selectin are constitutively expressed on BM endothelial cells,[20-22] and intravital studies have revealed that migration of HSPCs to BM occurs at specialized microvascular beds where E-selectin is expressed.[23] In another study, P-selectin–coated devices were shown to exhibit a sixfold enrichment of human $CD34^{pos}$ HSPCs over anti-CD34 antibody-coated devices, implying the importance of P-selectin for binding HSPCs.[24,25] BM transplantation studies into lethally irradiated mice lacking both endothelial selectins revealed that these mice exhibited a substantial defect in HSPC homing and a reduced survival that was rescued following the expression of either E- or P-selectin.[26] These and several other independent lines of evidence have highlighted vascular-selectin–dependent interactions as central to the recruitment of HSPC to BM.[26-29] In the current study, we determine the link between CD34 expression and the concurrent hematopoietic activation that leads to its improved homing and whether these vascular selectins can explain the gap in our understanding of this process. We revealed a more defined role for CD34 as a vascular selectin ligand and showed that it has comparable affinity and functional performance to other selectin ligands on human HSPCs. These new findings add to our preexisting understanding of selectin ligand contributions toward hematopoietic cell migration in therapeutic settings.

Methods

Mass spectrometry analysis of cognate E-selectin ligands expressed on human HSPC-enriched cells

Recombinant E-selectin chimeric protein (E-Ig) was used to immunoprecipitate ligands from a lysate of HSPC-enriched cells (as described in the supplemental Materials and methods), and the resulting samples were separated on 4% to 20% sodium dodecyl sulfate–polyacrylamide gel electrophoresis; protein bands were visualized by SimplyBlue SafeStain (Invitrogen). These bands were then reduced, alkylated, and digested in the gel with sequencing grade modified trypsin (Promega); the resultant peptides were extracted using buffer containing (5% acetonitrile [VWR], 95% water, and 0.1% formic acid [Sigma-Aldrich]). Following extraction, peptides were dried to ~1 μL sample volumes using a speed vacuum, fractionated by nanoflow liquid chromatography, and analyzed using a LTQ Orbitrap mass spectrometer (all acquired from Thermo Scientific). Raw data were converted to Mascot generic format files and searched using the online Mascot database.

Parallel plate rolling assay of CD34 knockdown cells

CD34 small interfering RNA (siRNA) was predesigned by Ambion silencer select (Applied Bioscience). For each nucleofection, 1×10^7 cells were pretreated with bromelain (500 μg/mL, 20 minutes at 37°C), washed with phosphate-buffered saline, gently resuspended in SE buffer mix (Amaxa) containing 500 nM of CD34-targeting (referred to as CD34-knockdown [KD]) or nontargeting control (scrambled), and then pulsed with the program EO-100 using a 4D-Nucleofector system (Amaxa). CD34 expression in CD34-KD and scrambled nucleofected cells were monitored routinely after 48 to 72 hours to be eligible for experimental use. For the cell binding assay, 1×10^6 CD34-KD or scrambled cells were suspended in Hanks balanced salt solution with 10 mM *N*-2-hydroxyethylpiperazine-*N*′-2-ethanesulfonic acid and 2 mM $CaCl_2$ and then perfused over an 80% confluent monolayer of Chinese hamster ovary cells expressing E-selectin (CHO-E) at 0.3 dyne/cm^2 for 60 seconds followed by stepwise increases every 15 seconds to a maximum of 4.2 dynes/cm^2, as previously described in Wiese et al.[30]

Hydrodynamic flow analysis of selectin and ligand binding by surface plasmon resonance

Surface plasmon resonance (SPR) binding experiments were performed using the Biacore T-100 system (GE Healthcare) at 25°C. Immobilization of monoclonal antibodies (mAbs) on a carboxy-methylated-5 dextran sensor chip was performed using an amine coupling kit (BIAcore) as described in supplemental Materials and methods to achieve immobilization level of mAbs between 4000 and 8000 response units (RU). Binding experiments were performed at a flow rate of 20 μL/min in running buffer (1% Triton X-100, 50 mM NaCl, 50 mM Tris-base, and 1 mM $CaCl_2$) for E-selectin or running buffer (0.05% P20, 150 mM NaCl, 2 mM $CaCl_2$, 50 mM Tris-base pH 8.0) for P-selectin, unless otherwise stated. Whole cell lysates were prepared in buffer containing (1% Triton X-100 in 250 mM NaCl, 50 mM Tris-HCl; pH 7.4, 20 μg/mL phenylmethylsulfonyl fluoride, and protease inhibitor cocktail tablet [Roche]) as described in the supplemental Materials and methods. These lysates were perfused over immobilized mAb, washed with the respective running buffer for at least 3 minutes to remove multiligand complex contamination, and then a standard concentration of E-Ig (177 nM; diluted in the running buffer) was injected for 130 seconds, unless otherwise specified. To correct for the buffer bulk refractive index and nonspecific interactions with the surface and with the mAb, a control flow cell immobilized with an equal amount of the mAb-corresponding isotype was used. For more details about the surface regeneration procedure, glycoprotease experiments, and calculations used to determine the dissociation binding constant, K_D, the dissociation rate constant (k_{off}) of the mAb·captured-ligand complex, the apparent dissociation rate constant ($k_{off\text{-}apparent}$) of the interaction of mAb·captured-ligand with E-Ig from a single concentration-type binding study, or the apparent association rate constant from multiple concentration-type binding study ($k_{on\text{-}apparent}$), please refer to the supplemental Materials and methods.

Statistical analysis

Data are expressed as the means ± standard error. Statistical significance of differences between means was determined by 1-way analysis of variance. If means were shown to be significantly different, multiple comparisons were performed post hoc by the Tukey *t* test. Statistical significance was defined as $P < .05$.

Additional materials and methods and details of the cells, enzymes, and reagents used are outlined in supplemental Materials and methods.

Results

$CD34^{pos}$ HSPC-enriched fractions from human BM express more E-selLs than $CD34^{neg}$ HSPC-enriched fractions

Given the requisite expression of E-selectin on BM endothelial cells for HSPC migration and trafficking,[23] we sought to compare the

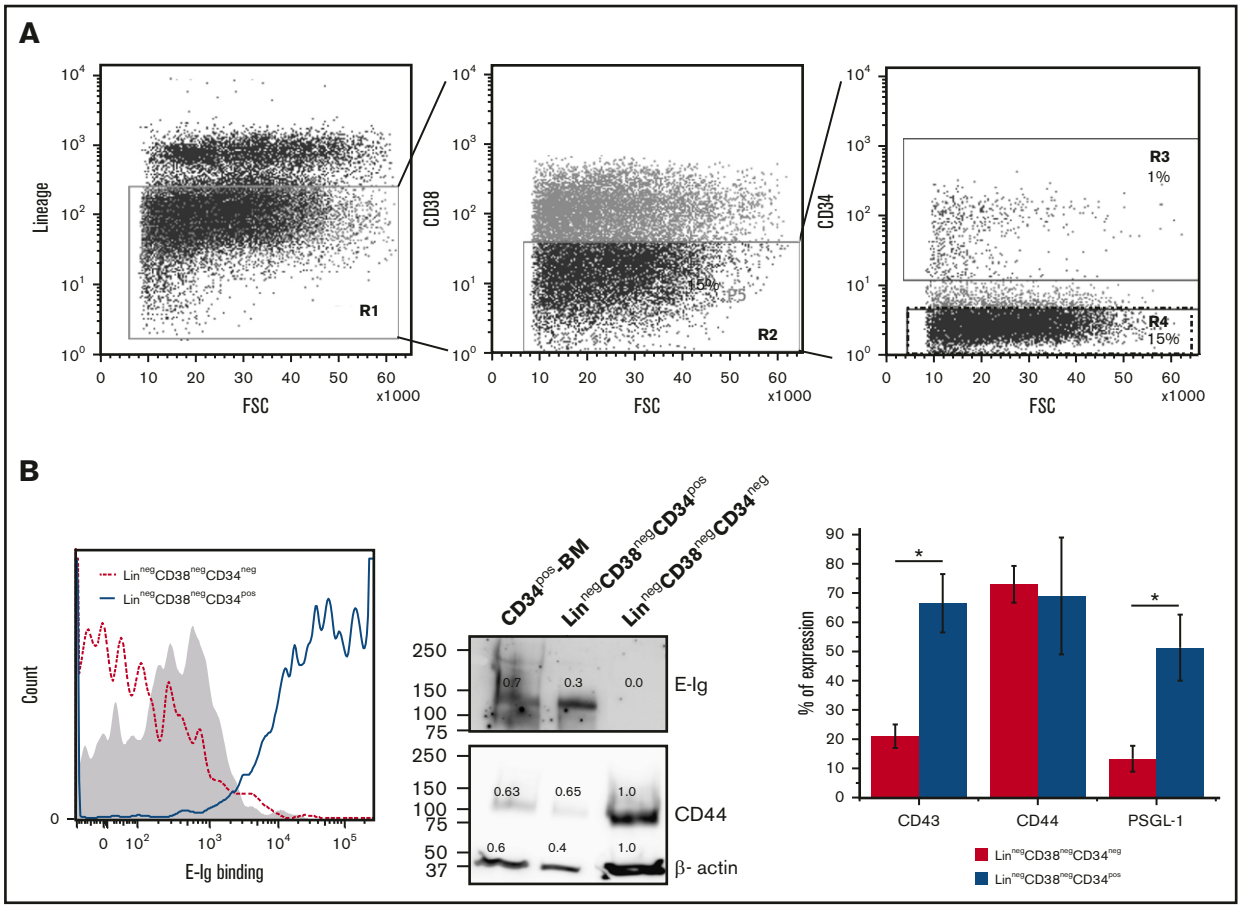

Figure 1. Differential expression of E-selLs on CD34^{pos} and CD34^{neg} subsets isolated from the Lin^{neg} CD38^{neg} fraction of human BM. (A) Overview of the gating strategy used to isolate CD34^{neg}CD38^{neg} and CD34^{pos}CD38^{neg} fractions by fluorescence-activated cell sorting of lineage-depleted (Lin^{neg}) BM MNCs. Left panel, dot plot represents the cell surface expression of a lineage marker cocktail (including CD2, CD3, CD11b, CD14, CD15, CD16, CD19, CD56, CD123, CD235a, and CD7). Cells residing in the negative fraction (R1) were further gated for CD38-negative cells (R2) (middle panel) and then subdivided into 2 subpopulations based on CD34 expression, CD34^{pos} and CD34^{neg} residing in R3 and R4 gates, respectively (right panel). Data shown are representative of n = 4 experiments. (B) Left panel, representative E-Ig staining profile of CD34^{pos} and CD34^{neg} subpopulations isolated as depicted in panel A. The shaded curve shows EDTA control (20 mM; on the Lin^{neg}CD38^{neg}CD34^{pos} subset), whereas dotted red and solid blue curves show the specific binding of CD34^{neg} and CD34^{pos} subsets, respectively (n = 4). Middle panel, lysates of CD34^{pos} BM cells (CD34^{pos}-BM), Lin^{neg}CD38^{neg}CD34^{pos}, and Lin^{neg}CD38^{neg}CD34^{neg} populations isolated from human BM were normalized for total protein level and subjected to western blot analysis. Membranes were blotted with E-Ig, CD44, or β-actin followed by isotype-matched HRP-conjugated mAb for visualization. This is representative of n = 4 independent experiments. Supplemental Figure 1 shows western blots where CD44 was immunoprecipitated from these cell populations and blotted with E-Ig, CD44, and HECA-452. Right panel, flow cytometric analysis of E-selLs expressed on the 2 subpopulations isolated as in panel A is shown as the average percent of expression (above the isotype control) of n = 3 independent experiments. *$P < .05$ relative to CD34^{neg} subpopulation. NIH Image J was used to quantify the intensity of western blot bands using the gel analyzer tool; the number displayed represents the density of each band related to the Lin^{neg}CD38^{neg}CD34^{neg} band as a standard. FSC, forward scatter.

ability of a recombinant E-selectin chimeric protein (E-Ig) to bind HSPC-enriched fractions either expressing CD34 (CD34^{pos}) or not (CD34^{neg}) that were isolated from human BM that was first depleted of lineage committed cells, including those cells expressing CD38 (Lin^{neg} CD38^{neg}). As expected, we found more CD34^{neg} than CD34^{pos} cells (15% vs 1%, respectively), which is in accordance with previous studies[5,31] (Figure 1A). Flow cytometric analysis comparing the Lin^{neg}CD38^{neg}CD34^{pos} to Lin^{neg}CD38^{neg}CD34^{neg} fractions showed higher E-Ig staining to the CD34^{pos} population than to the CD34^{neg} population (Figure 1B left panel). The positive population displayed a higher amount of E-selectin ligands (E-selLs) relative to the negative population after normalizing the slight differences in the amount of β-actin loaded as a control (Figure 1B middle panel). Note that CD34^{pos}-BM cells (isolated from mononuclear cells [MNCs] of human BM using only anti-CD34 microbeads alone; ie, not Lin^{neg} CD38^{neg}) express a range of E-selLs from ~100 to 250 kDa, whereas the Lin^{neg}CD38^{neg}CD34^{pos} cells express ligands at a molecular weight (MW) just over 100 kDa primarily (Figure 1B middle panel). The protein concentration of each extract was normalized using a bicinchoninic acid assay and β-actin staining (Figure 1B middle panel). To determine whether the difference in E-Ig staining between CD34^{pos} and CD34^{neg} was due to differential expression of E-selectin protein ligands, the expression of the common E-selLs expressed on HSPCs, including CD44, PSGL-1, and CD43,[32-34] was analyzed using flow cytometry. As shown in Figure 1B right panel, CD44 was expressed on both populations. Western blot analysis of the whole-cell lysates further confirmed that although CD44 expression in the CD34^{neg} fraction

Table 1. Summary of potential E-selLs expressed on CD34^{pos}-BM cells identified by MS

Description	Probability	Coverage of peptide sequence, %	Peptide sequence
CD34	1	9.6	LGILDFTEQDVASHQSYSQK,TSSC[160]AEFKK,LGILDFTEQDVASHQSYSQK, TSSC[160]AEFK, DRGEGLAR
Galectin-9B	.9997	7.3	FEDGGYVVC[160]NTR SIILSGTVLPSAQR
Galectin-9	.9998	7	FEDGGYVVC[160]NTR
CD44/HCELL	1	5.8	LVINSGNGAVEDR SQEM[147]VHLVNK NLQNVDM[147]K
Galectin-3	1	5.6	ASHEEVEGLVEK LADGGATNQGR AVDTWSWGER
CD43	.9996	4.5	TGALVLSR
Integrin β-2	1	3.9	TTEGC[160]LNPR YNGQVC[160]GGPGR SSQELEGSC[160]R
PSGL-1	.9907	2.2	SPGLTPEPR
Fms-related tyrosine kinase 3 ligand cytokine receptor	.9977	1.6	EMDLGLLSPQAQVEDS
Integrin α-L	.9337	0.9	HGGLSPQPSQR

was higher, it did not display HECA-452 reactivity (supplemental Figure 1) or E-selL activity (Figure 1B middle panel). Thus, the CD44 expressed on the CD34^{neg} fraction is not hematopoietic cell E-/L-selectin ligand (HCELL) because it does not display HECA-452 reactive CD44 that binds E-selectin, whereas that expressed on the CD34^{pos} fraction did exhibit HCELL characteristics (supplemental Figure 1).[32,35] Other known E-selLs (CD43 and PSGL-1) were expressed at low levels or absent (20% ± 4% vs 66.5% ± 24% for CD43 and 13% ± 4% vs 51% ± 11% for PSGL-1 positive cells in CD34^{neg} and CD34^{pos} populations, respectively; $P < .05$) (Figure 1B right panel). Overall, these results support that E-selectin binding is more pronounced on the CD34^{pos} fraction than on the CD34^{neg} fraction in part due to the differential expression of E-selLs between these 2 populations.

E-selectin binds CD34 expressed on human HSPC-enriched

To fully elucidate all noncanonical E-selLs expressed on CD34^{pos} HSPC-enriched cells from the BM (Figure 1B middle panel), we used a mass spectrometry (MS)–based proteomics approach. Among the several hundred ligands recognized by MS with a P value < .01, our dataset verified the presence of CD44, CD43, and PSGL-1, 3 well-known HSPC E-selLs (Table 1).[32-34] Furthermore, MS data analysis identified CD34, a ligand previously identified on KG1a cells to bind E-selectin in a parallel plate flow setting,[17] as a potential ligand on HSPCs. To validate the binding activity of CD34 to E-selectin, CD34 immunoprecipitates were prepared from lysates of CD34^{pos} fractions from normal umbilical cord blood (CD34^{pos}-UCB) and BM (CD34^{pos}-BM) as well as from acute myeloid leukemic (AML) cells (KG1a cell line and BM from AML patient [CD34^{pos}-AML]), all of which had been normalized for protein concentration. Western blots of these immunoprecipitates probed with E-Ig (1 μg/mL, n = 3) revealed a 120-kDa band in all samples tested, confirming that CD34 isolated from HSPC-enriched cells bound E-selectin (Figure 2A). Consistently, results from the reverse experiment verified that CD34 bound E-selectin (Figure 2B). MS analysis of CD34 immunoprecipitates from lysates of KG1a cells and CD34^{pos} human BM cells confirmed that the primary protein immunoprecipitated with the CD34 antibody is indeed CD34 without any contamination of other proteins (supplemental Table 1; supplemental Figure 2). Furthermore, an exhaustive immunoprecipitation with E-Ig (6 rounds) was performed on each of these cell types. Following the clearance of E-Ig reactive bands, the residual lysate was immunoprecipitated with the anti-CD34 mAb, QBend-10, to remove any leftover CD34 protein that was not removed by the E-Ig immunoprecipitations. Western blots were stained for CD34 and revealed the presence of a CD34 glycoform that was not bound by E-Ig in lysates from AML samples (Figure 2C); this glycoform was not present in lysates from normal cells. In addition, this glycoform lacked expression of sialyl Lewis x (sLe^x), which is essential for E-selectin binding (Figure 2D). Finally, confocal microscopy was used to further confirm the interaction of CD34 (CD34-mAb; red) and E-selectin (E-Ig; blue) on KG1a cells that were either pretreated with E-Ig for 1 hour or left untreated (Figure 2E). Using the Imaris Coloc analysis tool, we observed that CD34 appeared to colocalize with E-Ig (Figure 2E). Interestingly, CD34 appears to colocalize into clusters following a short exposure to E-Ig, suggesting that CD34 may be recruited to lipid rafts following exposure to E-Ig. Indeed, staining with lipid raft markers (CTB, green) indicated that E-Ig induced lipid raft formation and recruited CD34 to lipid rafts after E-Ig binding (Figure 2E). It should be noted that incubation of cells with E-Ig resulted in increased aggregation of cells (supplemental Figure 3). Furthermore, a confocal analysis following staining of CD34^{pos}CD38^{neg} lineage-depleted BM cells from AML and normal BM with E-Ig (E-selectin), HECA-452 (sLe^x), and 8G12 (CD34 protein) revealed that CD34^{pos} AML cells from the BM (Figure 2F lower panels) express a CD34 glycoform that does not bind E-selectin or express sLe$^{x/a}$ epitopes, whereas CD34^{pos} from normal BM (Figure 2F upper panels) counterparts do not; this is indicated by the yellow arrows in lower panels of Figure 2F. These data reinforce the data presented in Figure 2C-D, indicating that a unique glycoform of CD34 exists in AML samples that does not appear to be present in normal samples.

CD34 is an E-selL under flow conditions

To examine whether native CD34 on human HSPC-enriched populations displayed functional E-selL activity in flow-based assays, we employed 3 approaches: the SPR-based binding assay developed in our laboratory,[36] the Stamper-Woodruff assay,[37] and the blot-rolling assay.[38,39] We compared CD34 binding to the well-established E-selL, CD44 (ie, HCELL).[32,35] The real-time binding feature of our SPR assay enabled us to isolate endogenously

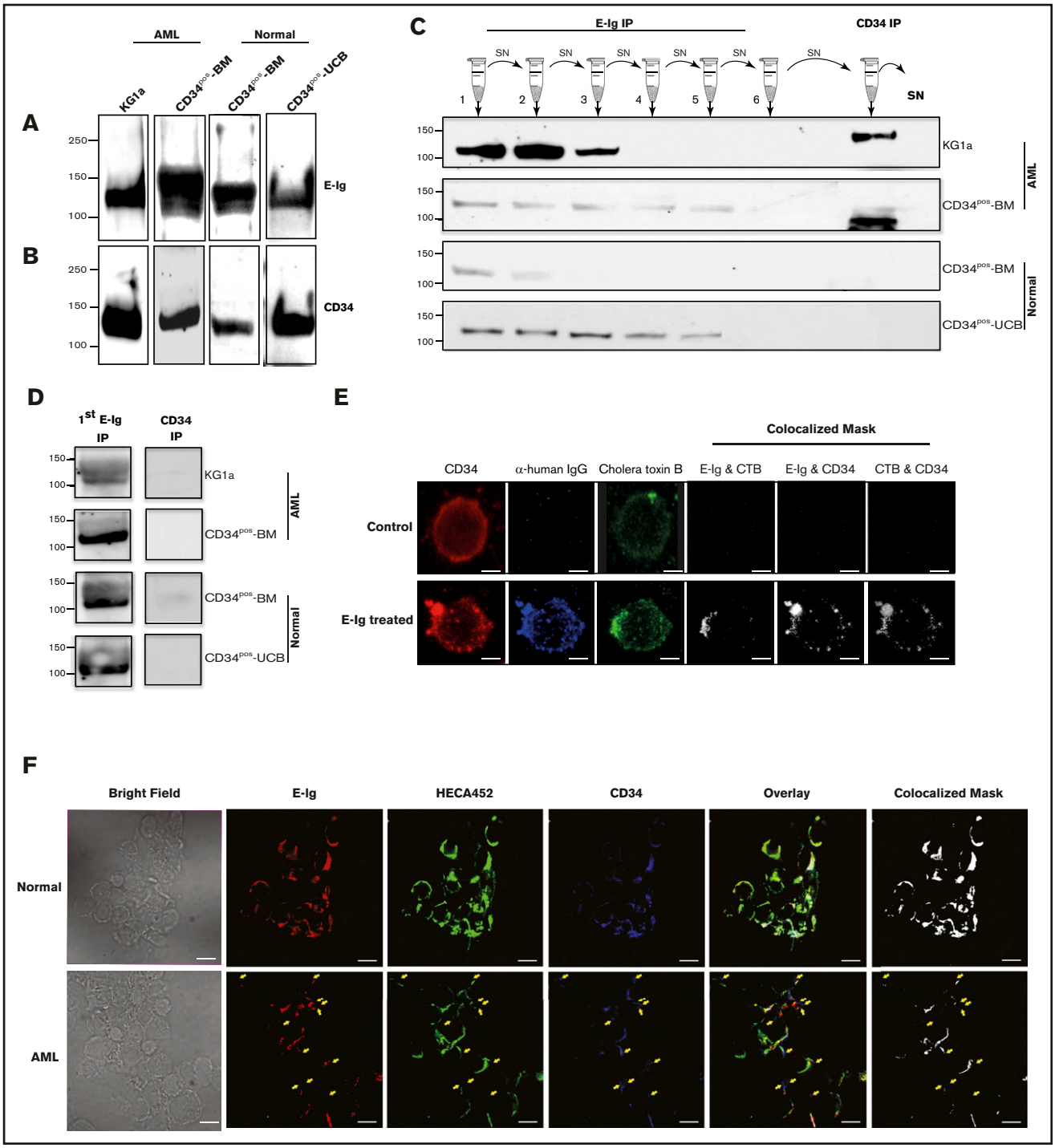

Figure 2. The sialomucin CD34 is a novel ligand for E-selectin. (A) CD34 was immunoprecipitated from HSPC-enriched lysates of CD34^{pos} cells isolated from normal UCB cells (CD34^{pos}-UCB), normal BM cells (CD34^{pos}-BM), AML BM cells (CD34^{pos}-AML), or KG1a cells (n = 3 patient samples and KG1a cells). Lysates were subjected to western blot analysis with E-Ig chimera. This is a representative blot of n = 3 experiments. (B) The reciprocal immunoprecipitation assay was performed where E-Ig chimera was used first for immunoprecipitation prior to western blot analysis using CD34 QBend-10 mAb (n = 3). (C-D) AML cells express a unique form of CD34 that does not function as an E-selL. Multiple rounds of E-Ig immunoprecipitations were performed on both normal and AML sample cell lysates, and following the clearance of E-Ig reactive bands, the residual lysates were immunoprecipitated using QBend-10 (CD34-mAb that recognizes all classes of CD34) and subjected to western blot analysis for CD34 (QBend-10) (C) and anti-sLe^{x} (HECA-452) (D). SN = supernatant. For panel D, as described in the supplemental Materials and methods, only the first elution after E-Ig immunoprecipitation and the CD34 immunoprecipitation are shown. These blots are representative of n = 4 separate experiments. (E) KG1a cells were pretreated with E-Ig chimera or left untreated prior to lipid raft staining with choleratoxin-β (CTB)-AF-594 (green). Fixed cells were then stained with CD34 (Cy5; red) and AlexaFluor-488 streptavidin (blue) toward biotinylated anti-human-Ig to detect E-Ig. The colocalized mask was analyzed using Imaris Coloc software. Cell surface labeling with an isotype control

expressed CD34 and CD44 from human HSPC-enriched lysate and then measure their direct binding to recombinant E-Ig. Ligand-specific mAbs (4H11 for CD34 and Hermes-3 for CD44) or isotype controls (mouse immunoglobulin [MsIgG]) were first immobilized on a carboxy-methylated-5 sensor chip. Following the injection of the HSPC-enriched lysate, significant RU accumulated in the CD34 and CD44 flow cells, whereas only residual RUs were detected in the control flow cells that were either left blank (no mAb) or were immobilized with isotype control (MsIgG) (Figure 3A). It should be noted that the CD44 mAb used here captured a mixture of CD44 glycoforms[36] of which only a fraction bound E-selectin. Furthermore, the purity of the captured CD34 was assessed as described previously.[36] Briefly, following lysate injection, a 5-minute buffer-washing step was introduced in order to eliminate potential multiligand complexes. Captured proteins were recovered and then subjected to western blot analysis as detailed in supplemental Materials and methods. Immunostaining with CD34-mAb verified the presence of CD34 (Figure 3A inset), whereas immunostaining for the presence of PSGL-1, a highly expressed E-selL on hematopoietic cells,[33,34,36] verified its absence (Figure 3A inset). As estimated from Equation 1 in supplemental Materials and methods, we observed low ligand-capturing efficiency, likely attributed to the immobilization of the mAb rendering its binding site inaccessible, with only 9.5% and 20.2% for CD34 and CD44, respectively. The values used in these calculations for the maximum RU reached at the end of the lysate injection (RU_{max}) for CD34 and CD44 were 546 and 559, respectively (Figure 3A), and the apparent MWs for mAb, CD34, and CD44 were nearly 150, 120, and 80 kDa, respectively. Next, we examined the binding of CD34·4H11-mAb and CD44·Hermes-3-mAb complexes with E-selectin. Results in Figure 3A represent the raw data before subtracting the buffer bulk refractive index and residual nonspecific interactions using a flow cell with the isotype control, whereas Figure 3B shows the subtracted sensorgrams that were subsequently normalized based on the difference in the ratio of the captured CD34 and CD44 just before E-Ig injection. We observed an 8.6-fold faster dissociation rate constant (k_{off}) during the washing step for captured CD34 relative to CD44 from the mAb complex (Figure 3B). To assess the specificity of this interaction, we injected E-Ig (177 nM) in the presence of EDTA (5 mM) and confirmed that no interaction occurred in either complex. A marked increase in RU was detected when E-Ig was injected in the presence of Ca^{2+} (Figure 3B) with no or minimal binding to either isotype or blank controls (Figure 3A). The apparent dissociation rate constant ($k_{off\text{-}apparent}$), which consists of the dissociation of CD34 or CD34·E-Ig from 4H11-mAb as well as the dissociation of E-Ig from CD34·4H11-mAb, was 3.3×10^{-4} s^{-1} (Figure 3B).

Immunoprecipitations of CD34 from both $CD34^{pos}$-BM cells and KG1a cells also supported the presence of adhesive interactions observed with CHO-E cells in Stamper-Woodruff assays displaying 14 ± 2 bound cells to CD34 isolated from $CD34^{pos}$-BM and 26 ± 2 bound cells to CD34 isolated from KG1a; no binding was observed in the presence of EDTA (Figure 3C). Moreover, using blot-rolling assays of HECA-452 stained blots of E-selL immunoprecipitates, we observed that CD34 supported significant rolling of CHO-E cells under physiological shear stress in addition to the well-known E-selLs (CD44, CD43, and PSGL-1) immunoprecipitated from the human KG1a cell lysate (Figure 3D). CD43 supported the least amount of CHO-E rolling of all the ligands tested. Specificity for E-selectin binding was confirmed by the elimination of binding in the presence of EDTA or by using mock-transfected CHO cells (CHO-M) (Figure 3D). Overall, these multiple binding studies revealed that CD34 is a relevant and functional E-selL that may cooperate with other E-selLs in directing human HSPCs to E-selectin expressing sites.

The equilibrium dissociation binding constants of E-selectin to CD44, CD34, and PSGL-1 were relatively similar but varied in their binding stoichiometry

Next, we directly compared the binding affinities of E-selLs (CD44, CD34, CD43, and PSGL-1) expressed on KG1a cells by consecutive E-Ig injection at a physiological NaCl concentration (150 mM) using the SPR-based immunoprecipitation assay. During 5 minutes of washing at 20 μL/min, captured CD34 and CD43 continuously dissociated from their mAbs such that the amount of protein collected decreased by 20% to 25% (Figure 3B). This created an unreliable estimate of the dissociation binding constant (K_D). Therefore, the CD34 563-mAb and CD43·polyclonal-Ab complexes were covalently linked by including another run of amine coupling that comprised injecting a 1:1 mix of N-hydroxysuccinimide:1-ethyl-3-(3-dimethylaminopropyl) carbodiimide hydrochloride (NHS:EDC) for 350 seconds followed by deactivation with ethanolamine for 400 seconds at 5 μL/min. Using a steady-state model, K_D, $k_{off\text{-}apparent}$, and the apparent association rate constant ($k_{on\text{-}apparent}$) were calculated for E-selLs (Figure 4A; Table 2). We observed that CD34, CD44, and PSGL-1 bound to E-Ig similarly with K_D of 236.7 ± 38, 233 ± 9, and 259 ± 34 nM, respectively, values that are nearly half of that for CD43 (442 ± 47 nM) (Table 2). These results are consistent with the results of the blot-rolling assay, where the numbers of CHO-E cells rolling over CD43 immunoprecipitates were significantly reduced ($P < .05$; Figure 3D).

Assuming 1:1 stoichiometry, the percentage of active E-selLs that bound E-Ig was derived from the binding isotherms of their interactions (Figure 4A; Table 2) and was found to be $54\% \pm 17\%$, $23.0\% \pm 0.3\%$, $19\% \pm 2\%$, and $75\% \pm 3\%$ for CD34, CD44, CD43, and PSGL-1, respectively. These percentages could, however, be upper estimates because we did not rule out the possibility that each ligand could bind >1 E-Ig molecule. Although E-Ig bound E-selLs with similar intrinsic binding behavior

Figure 2. (continued) or a secondary antibody alone served as background controls (data not shown). Results are representative of n = 3 independent experiments, 7 fields per experiments; >5 cells per field. Scale bar is 5 μm. (F) $CD34^{pos}$ cells from AML BM (lower panels) express a CD34 glycoform that does not bind E-selectin, whereas $CD34^{pos}$ from normal BM (upper panels) counterparts does not. $CD34^{pos}CD38^{neg}$ lineage-depleted BM cells from either AML or normal BM were prepared for confocal analysis and stained for E-selectin chimera (E-Ig; red), sLe^x expression (HECA-452; green), and CD34 (8G12; blue). Bright field images are also shown. Colocalization analysis was performed using Imaris 7 software to construct the colocalization mask (white). Yellow arrows in the AML images (lower panels) point to spots where CD34 expression is not overlaid with E-selectin binding or sLe^x expression. Results are representative of n = 3 independent experiments. Scale bar is 10 μm. For clarity, panels A-D were performed on $CD34^{pos}$ samples from normal or AML BM wherever stated and panel F was performed on $Lin^{neg}CD38^{neg}CD34^{pos}$ cells from normal or AML BM. IP, immunoprecipitation.

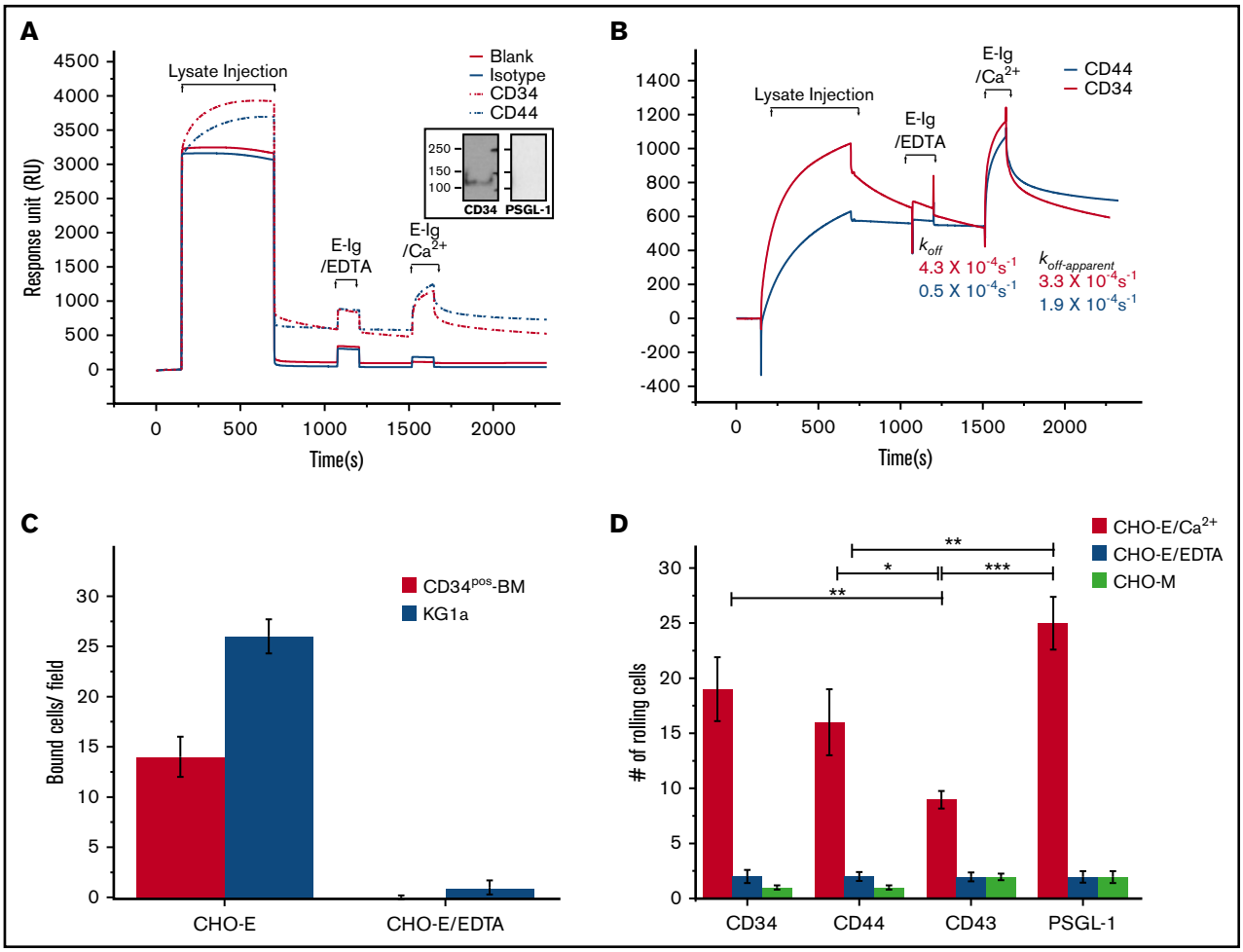

Figure 3. Flow-based binding assays confirm that CD34 is a functional E-selL. (A) Raw data depicting the capturing of E-selectin ligand from KG1a lysate on surface-immobilized antibodies and their subsequent binding to E-selectin by SPR. The lanes of the flow cell represent blank (red line), immobilized CD34-mAb (4H11) (7360 RU; red dashed line), immobilized CD44-mAb (Hermes3) (5200 RU; blue dashed line), and immobilized isotype control (4377 RU; blue line). The mAb immobilization (step 1) is not shown. Lysate injection, arrows mark the start and end of the lysate injection, which is then followed by a buffer washing step. The sensorgrams represent the raw data of the uncorrected RU for the buffer bulk refractive index and nonspecific interactions. Inset, western blot analysis and staining for either CD34 (left panel) or PSGL-1 (right panel) after eluting them from the chip confirming specificity of their capturing by SPR. E-Ig/EDTA injection, the injection involves E-Ig (177 nM) in the presence of EDTA (5 mM) as a control to show specificity of E-Ig to its ligands. E-Ig/Ca^{2+} injection, the injection involves Ca^{2+} (1 mM) to support E-Ig (177 nM) binding to its ligands. (B) Corrected sensorgrams for the buffer refractive index and nonspecific interactions. Data were presented as described in panel A but after subtracting the RU of the buffer refractive index and nonspecific interactions from the standard reference flow cell that contains the isotype control. Furthermore, normalization was applied to even out the difference in the level of mAb-captured CD34 and CD44 as described in the supplemental Materials and methods. k_{off} is the dissociation rate constant for CD34 and CD44 from their respective mAb, and $k_{off\text{-}apparent}$ is the apparent dissociation rate constant for E-Ig, CD34/E-Ig, or CD44/E-Ig from their respective mAb as well as E-Ig from the complexes CD44·Hermes-3-mAb or CD34·4H11-mAb (n = 3 independent experiments). (C) Immunoprecipitations of CD34 were prepared from lysates of $CD34^{pos}$-BM and KG1a cells and spotted on glass slides to test for CHO-E binding using a Stamper-Woodruff assay. Adherent CHO-E cells were counted by light microscopy using an ocular grid under magnification ×20. The data are representative of 1 experiment, and the error bars indicate the standard error of the mean (SEM) of 7 fields per slide on 2 slides for each experiment (n = 3 independent experiments). (D) Blot-rolling assays were performed on western blots of CD34, CD44, CD43, and PSGL-1 immunoprecipitates from KG1a cells stained for HECA-452. CHO-E cells were subsequently perfused over immunoprecipitated glycoproteins at 0.25 dyne/cm^2. After cell perfusion, the numbers of rolling cells per field were counted (red bars). As a control, CHO-E cells incubated with EDTA (blue bars) or mock-transfected CHO cells (CHO-M) (light green bars) were used. Results shown reflect the average number of rolling cells over the HECA-452 blots of n = 7 membrane preparations from 4 distinct fields of view each. Data are mean ± SEM (error bars). *$P < .05$; **$P < .01$; ***$P < .001$.

(comparable $k_{on\text{-}apparent}$ and $k_{off\text{-}apparent}$), PSGL-1 and CD34 were found to express a significantly greater number of E-Ig binding sites than did CD44 or CD43, which could explain the rolling behavior of CHO-E over these ligands compared with rolling over PSGL-1 ($P < .05$ and $P < .001$, respectively; Figure 3D). These data suggest that PSGL-1 displayed the highest number of ligand active sites ($P < .001$ for CD44 and $P < .01$ for CD43) followed by CD34, CD44, and then CD43.

Further analysis of the E-selectin binding kinetics of CD34 extracted from primary cells was performed using $CD34^{pos}$-BM lysate.

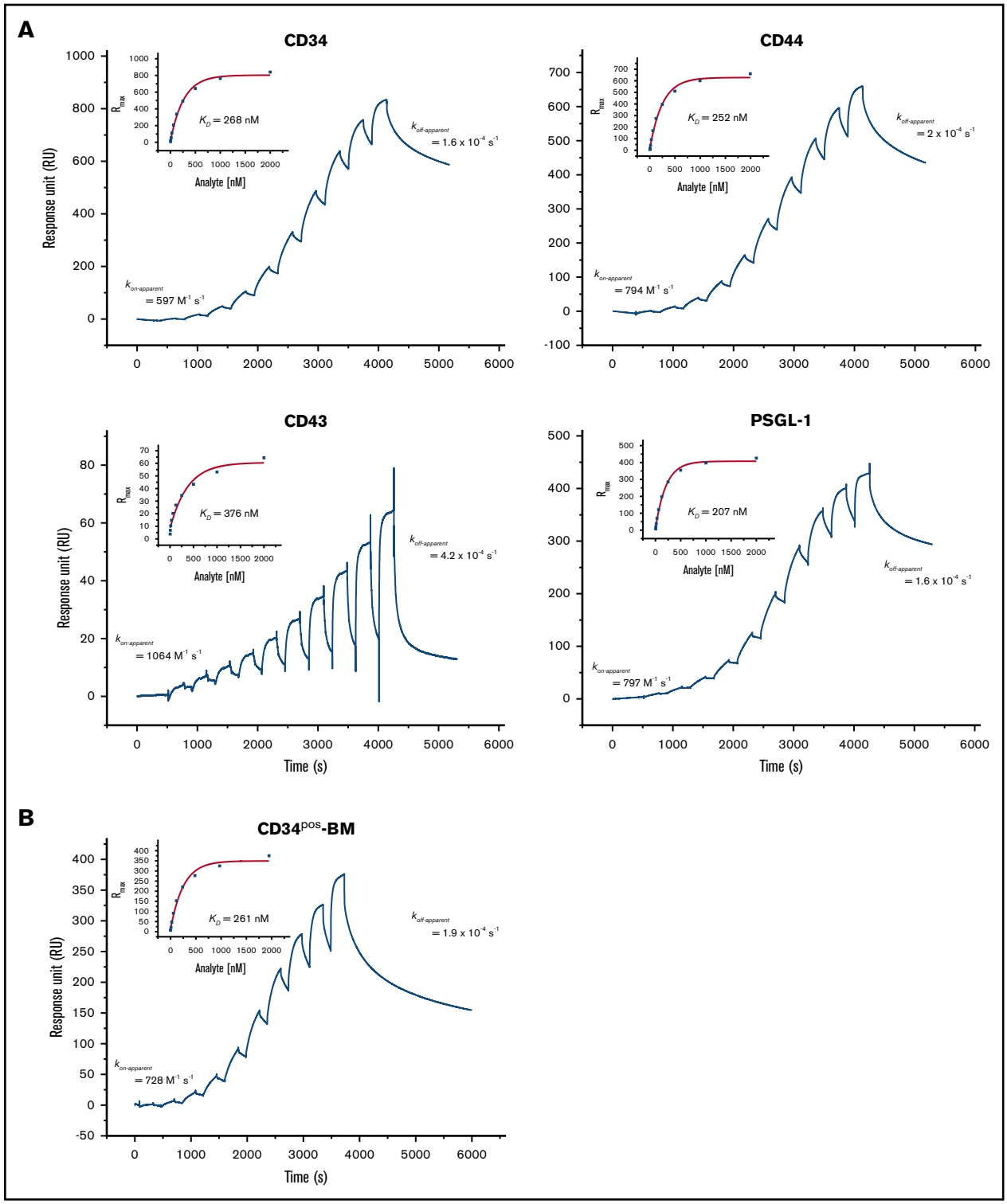

Figure 4. Determination of the dissociation binding constant (K_D) for the binding of E-selLs from HSPC-enriched lysates to E-Ig. The sensorgrams show binding of consecutive injections of E-Ig at 15 μL/min for 240 seconds each at concentrations of 3.9, 7.8, 15.6, 31.3, 62.5, 125, 250, 500, 1000, and 2000 nM that are each spaced by a 60-second buffer washing step (A) over captured E-selLs (CD34, CD44, CD43, and PSGL-1) expressed in KG1a cell lysate (150 mM NaCl) and (B) over captured CD34 from $CD34^{pos}$-BM lysate (50 mM NaCl). 563-mAb (10 800 RU for KG1a lysate or 6952 RU for $CD34^{pos}$-BM lysate) or $MsIgG_1$ isotype control (8320 RU for KG1a and 7500 RU for $CD34^{pos}$-BM lysate) was immobilized to capture CD34 (left upper panel). Hermes-3-mAb (9300 RU) or $MsIgG_{2a}$ isotype control (7700 RU) was immobilized to capture CD44 (right upper panel). KPL-1-mAb (11 400 RU) or $MsIgG_1$ isotype control (8090 RU) was immobilized to capture PSGL-1 (right lower panel). A polyclonal CD43 Ab (15 800 RU) or Goat isotype control (14450 RU) was immobilized to capture CD43 (left lower panel). The sensorgrams presented are corrected for the bulk refractive

Table 2. Summary of affinity and kinetic values for E-Ig binding to E-selLs: CD34, CD44, CD43, and PSGL-1 using a SPR-based assay

	CD34				CD44			
	1st	2nd	3rd	Mean ± SEM	1st	2nd	3rd	Mean ± SEM
K_D, nM	145	268	297	236.7 ± 38	234	252	214	233 ± 9
$k_{off\text{-}apparent}$, s^{-1}	2.90E−04	1.60E−04	3.31E−04	2.6E−4 ± 0.4E−4	1.10E−04	2.00E−04	2.73E−04	1.9E−4 ± 0.4E−4
$k_{on\text{-}apparent}$, M^{-1} s^{-1}	2030	597	1054	1230 ± 346	641	794	1280	903 ± 156
	CD43				PSGL-1			
	1st	2nd		Mean ± SEM	1st	2nd	3rd	Mean ± SEM
K_D, nM	508.7	376		442 ± 47	342.5	207	229	259 ± 34
$k_{off\text{-}apparent}$, s^{-1}	4.80E−04	4.20E−04		4.5E−4 ± 0.2E−5	1.50E-04	1.65E−04	2.62E−04	1.9E−4 ± 0.3E−4
$k_{on\text{-}apparent}$, M^{-1} s^{-1}	944	1063.8		1004 ± 43	438	797	1144	793 ± 166

Because of the relatively low protein concentration in these cell lysates, limited amounts of CD34 (172 RU, data not shown) were captured compared with that from the KG1a cell lysate. However, E-Ig binding still displayed a dose-dependent response with a K_D of 261 nM (Figure 4B). After the last E-Ig injection, $k_{off\text{-}apparent}$ was estimated to be 1.9×10^{-4} s^{-1}, which was very similar to that of the CD34 extracted from the KG1a lysate. Thus, $k_{on\text{-}apparent}$ of 728 M^{-1} s^{-1} was considered a reasonable estimate for CD34. Overall, these results demonstrated relative similarities between the binding affinities of CD34 with cells isolated from either primary $CD34^{pos}$-BM or KG1a cell lysates, displaying slow on-/slow off-rate kinetics.

CD34 silencing resulted in markedly faster rolling velocities at higher shear stresses likely due to reduction in microvilli

We used a parallel plate-rolling assay to directly measure the relative contribution of CD34 to the overall rolling behavior of HSPCs. Using a knockdown approach, we compared the ability of cells lacking CD34 (CD34-KD) and control cells (scrambled) to tether and roll over E-selectin-expressing cells. Changes in the phenotype and loss of the sLe^x epitope that are associated with native HSPCs knockdown cells[34] made it favorable to use the HSPC-like cell line KG1a. As measured by flow cytometry, siRNA nucleofection of KG1a cells resulted in a 50% reduction in the surface expression of CD34 relative to scrambled cells (geometric mean fluorescent intensity) (Figure 5A). Meanwhile, flow cytometry indicated that there were no changes in the expression of other E-selLs or in HECA-452 reactivity of CD34-KD cells compared with scrambled control, but a slight increase in E-Ig staining was observed in CD34-KD cells (Figure 5A). Western blots of equal amounts of loaded proteins revealed that CD34 expression was substantially reduced, correlating with a slight increase in both HECA-542 and E-Ig staining, especially at ~100 to 150 kDa; this observation was not due to an increase in the expression of any of the measured E-selLs (Figure 5B). We observed that although the number of rolling cells after perfusing scrambled control or CD34-KD over CHO-E cell monolayers did not vary under any shear stresses tested (Figure 5C), CD34-KD cells rolled markedly faster than did the control, especially at or above 3 dyne/cm^2 (postcapillary venule shear; $P < .05$; Figure 5D). Specificity for E-selectin binding was confirmed by treatment of CHO-E cells with a function-blocking mAb (data not shown). Interestingly, transmission electron microscopic (TEM) images comparing CD34-KD and scrambled control KG1a cells revealed a profound reduction in microvilli type structures following CD34 knockdown (Figure 5E). Moreover, the cells showing this reduction in microvilli and plasma membrane convolutions did not present with any other changes in their ultrastructures: the endoplasmic reticulum was intact and not swollen; the mitochondria were comparable to those of control cells; and the nuclear envelope was intact. These results indicate that CD34 plays a significant role in slowing down the rate at which KG1a cells roll, although it does not affect the number of interactions between KG1a cells and CHO-E cells and suggests that this may be due, in part, to its role in regulating microvilli structures.

CD34 binding to E-selectin is dependent on sialofucosylated *O*-glycans

L-selectin is well known to bind sulfated sLe^x (6-sulfo-sLe^x) capped *O*- and *N*-glycans of the CD34 core protein.[40] We performed both SPR-based immunoprecipitation assay and western blot analysis to determine the glycan modifications necessary for CD34 to bind E-selectin following treatment with the glycosidases: O-sialoglycoprotein endopeptidase (OSGE; to remove *O*-glycans), Peptide:N-Glycosidase F (PNGase F; to remove *N*-glycans), or neuraminidase (to remove sialic acid). To perform a quantitative comparative analysis, we normalized the amount of mAb-captured ligand in the control to that in the treated based on their RUs prior to E-Ig injection, as described in the supplemental Materials and methods. Sensorgrams of E-Ig (354 nM) binding to antibody captured CD34 (CD34·4H11-mAb) from either neuraminidase-treated or control lysates showed that binding is eliminated following sialic acid digestion (Figure 6A). Western blot analysis of treated CD34

Figure 4. (continued) index and nonspecific interactions using the isotype controls. K_D was determined by fitting the binding isotherm using a steady-state model and the RU_{max} values just prior to the start of the buffer injection where steady-state conditions were nearly met (inset) and $k_{off\text{-}apparent}$ as described in Figure 3B. Data are representative of n = 3 independent experiments.

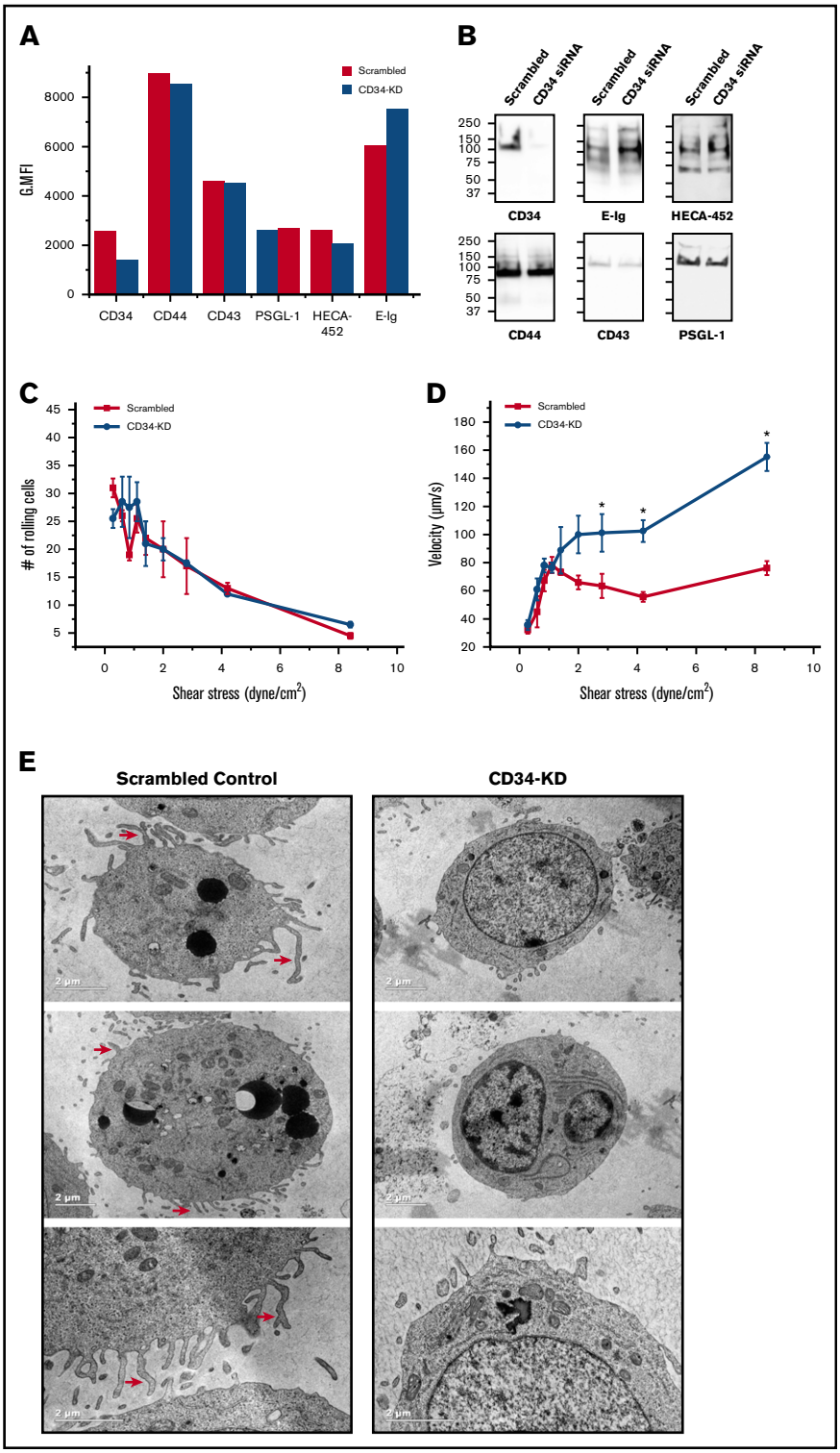

Figure 5. Silencing CD34 leads to a decrease in microvilli and higher rolling velocities with increasing shear stress. (A) Flow cytometric analysis of E-selL expression and E-lg and HECA-452 binding of scrambled and CD34 siRNA-nucleofected KG1a cells (CD34-KD). This is a representative figure of n = 4 independent experiments depicting the geometric mean fluorescent intensity (G.MFI). (B) Equivalent amounts of scrambled and CD34-KD cell lysates were subjected to western blot analysis and stained for CD34, CD44, CD43, PSGL-1, sLe^x (HECA-452), and E-lg. Blots are representative of n = 4 independent experiments. (C) Scrambled or CD34-KD KG1a cells were each perfused over CHO-E cell monolayers for 1 minute at 0.28 dyne/cm^2, and then detachment assays were employed by increasing the shear stress stepwise every 15 seconds. The average number of rolling cells in 4 distinct fields of view for each experiment (n = 4) was counted. (D) Single-cell tracking with Imaris V7.6.4 software was used to calculate KG1a rolling velocity over CHO-E cells from (C) at each shear stress depicted as described. The adhesion histogram is representative of n = 4 independent experiments, and data are reported as the mean ± SEM (error bars). *$P < .05$. (E) KG1a cells were either transfected with scrambled control siRNA (scrambled control) or with CD34 siRNA (CD34-KD), and 48 hours later, cells were fixed with glutaraldehyde and prepared for TEM analysis as outlined in supplemental Materials and methods. Red arrows point out some of the microvilli-type structures that are evident in the scrambled control but not in the CD34-KD images. These are representative cells of over 30 different cells imaged under each condition.

immunoprecipitates from KG1a or CD34^{pos}-UCB lysates verified SPR results (Figure 6B top panels). We evaluated the efficiency of neuraminidase to digest sialic acid using western blots and probing with the QBend-10 antibody (Class 2 mAb) to track the shift in the MW of CD34 from ~120 kDa to 150 kDa (Figure 6B lower panels).[36,41] To determine whether the E-selectin binding epitope resides on *N*- and/or *O*-glycans, we treated the KG1a lysate with PNGase F or OSGE, respectively. We found that removing the *N*-glycans resulted in only a small reduction in RU_{max} (1.4-fold) and a similar dissociation constant ($k_{off\text{-}apparent}$) as the control lysate (Figure 6C). By contrast, *O*-glycan removal completely abolished the interaction of E-lg with the CD34·4H11-mAb complex

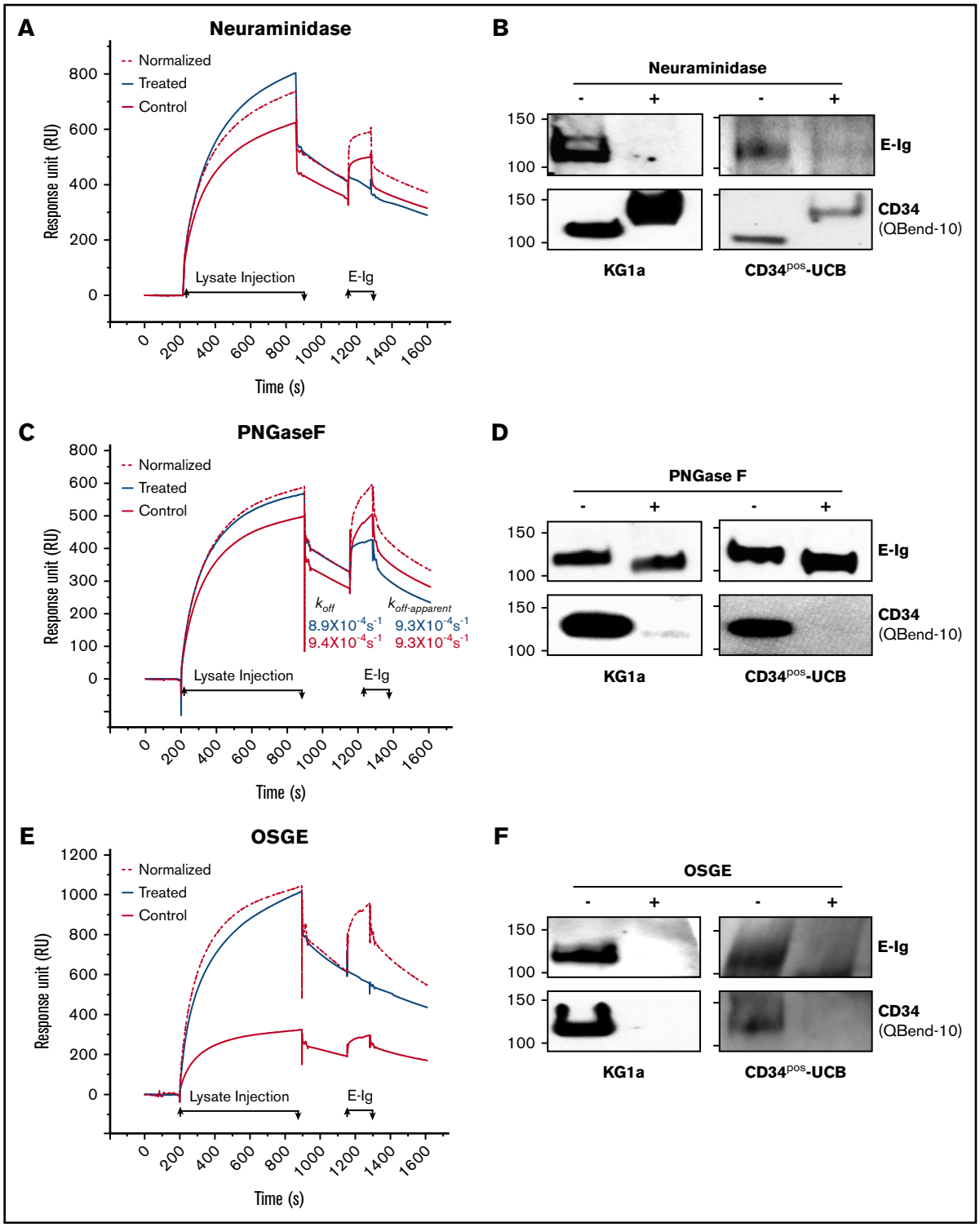

Figure 6. E-selectin binds predominantly to *O*-glycans on CD34. (A) 4H11-mAb (4964 RU) or its isotype control (4036 RU) were immobilized to capture CD34 from KG1a lysates that were treated with neuraminidase (Treated; blue line) or left untreated but subjected to the same buffer-treatment conditions, incubation times, and temperatures (Control; red line). Following CD34 capture, E-Ig was injected at 354 nM. The same surface was used for both the treated and the control binding studies with a surface regeneration step between the 2 runs. The normalized (red dashed line) sensorgram is the same as the control but normalized to the treated sensorgram based on the ratio of accumulated CD34 RU prior to E-Ig injection. (B) For western blot analysis, equivalent amounts of CD34 immunoprecipitates from HSPC-enriched lysates (KG1a or $CD34^{pos}$-UCB) were either treated with neuraminidase (+) or not (−) and blotted with either E-Ig (top panel) or CD34 (QBend-10, lower panel). Note that the apparent increase in MW of CD34 is attributed to the loss of the negatively charged sialic acid. (C) SPR analysis of the PNGase F treatment was performed as in panel A using 4H11-mAb (6500 RU) or its isotype control (5810 RU). k_{off} and $k_{off\text{-}apparent}$ were calculated as described in Figure 3B. (D) CD34 immunoprecipitates were treated with PNGase F

(Figure 6E); results were verified by western blot analysis (Figure 6D,F top panels). The glycoprotease-sensitive CD34-mAb, QBend-10, is sensitive to the removal of *O*- or *N*-linked glycans on CD34 and is therefore routinely used to detect the efficiency of glycan removal (Figure 6D,F lower panels).[36] These findings indicate that, in contrast to CD44 (ie, HCELL), which displays E-selL determinants on *N*-glycans and *O*-glycans,[32,36] CD34 presents sLe^x decorations mainly on *O*-glycans similar to CD43 and PSGL-1.[34,42]

P-selectin binds CD34 on sulfated *O*-glycans expressed on human HSPC-enriched cells

E- and P-selectin are expressed on human BM endothelial cells.[20,21] To date, the only ligand known to bind all 3 selectins (E-/P- and L-selectin) on HSPCs is PSGL-1.[33,43,44] In order to determine if CD34 on HSPCs is a P-selectin ligand, recombinant P-selectin human immunoglobulin chimeric protein (P-Ig) was used to immunoprecipitate P-selectin ligands from KG1a or CD34^{pos}-BM lysates, and subsequently western blots were stained for CD34 (EP373Y and QBend-10-mAb) or for PSGL-1 (KPL-1-mAb). CD34 and PSGL-1 were pulled out using P-Ig, and no PSGL-1 was found within the CD34 immunoprecipitate (Figure 7A). In addition, reciprocal studies also confirmed that CD34 and PSGL-1 immunoprecipitated from lysates of KG1a and CD34^{pos}-BM bound P-selectin (Figure 7B). Intriguingly, 2 MW forms (between 120 kDa and 130 kDa) of CD34 appeared to be able to bind P-selectin in the HSPC-enriched lysates (Figure 7B); therefore, to determine whether E-selectin recognizes the same CD34 glycoform as P-selectin, we eluted E-selLs following E-Ig immunoprecipitation of KG1a lysate using EDTA and subsequently immunoprecipitated this elution with CD34-mAb. As shown in Figure 7C, the higher MW form of CD34 (~130-kDa) is both an E- and a P-selectin ligand, denoting this MW glycoform of CD34 as a ligand that is able to bind both vascular selectins on HSPC-enriched cells. Furthermore, CD34 immunoprecipitated from CD34^{pos}-BM and KG1a cells supported CHO-P cell rolling (8 $\pm$ 2, compare with 41 $\pm$ 7 bound cells per field, respectively) using Stamper-Woodruff assays, whereas no binding was observed with the EDTA control (Figure 7D). Moreover, among the other E-selLs (CD34, CD44, CD43, and PSGL-1), only CD34 and PSGL-1 exhibited functional binding activity to CHO-P in blot-rolling assays (Figure 7E). Glycoprotease treatment of CD34 immunoprecipitates from KG1a cells revealed neither treatment with PNGase F nor with neuraminidase inhibited the binding of P-Ig to CD34, suggesting that *N*-glycans and sialic acid are not critical for P-selectin binding. Alternatively, OSGE treatment significantly reduced P-Ig staining, suggesting that *O*-glycans are essential for binding. To determine whether sulfation of CD34 is critical for P-selectin binding, we cultured KG1a cells in the presence or absence of chlorate, a metabolic inhibitor of the main sulfate donor on both tyrosine residues and glycoconjugates[45] prior to the preparation of cell lysates. As shown in Figure 7G, CD34 immunoprecipitates after chlorate treatment were not able to bind P-selectin compared with the control (left panel). Furthermore, CD34 immunoprecipitates treated with arylsulfatase, an enzyme that releases sulfates from tyrosine residues but not carbohydrates,[46,47] abrogated P-selectin binding to CD34 compared with the control (treated with buffer alone) (Figure 7G right panel). Complete cleavage of sulfated tyrosine residues was confirmed by the loss of anti-PSGL-1-mAb, KPL-1epitope (Figure 7G middle panels), which recognizes the tyrosine-sulfated motif without affecting the overall amount of PSGL-1 protein recognized by PL-2 (data not shown) or the CD34 protein level recognized by QBend-10-mAb following treatment (Figure 7D lower panels).[46] In summary, these data imply that unlike PSGL-1 binding to P-selectin, which requires sialylated glycans,[47,48] the binding of CD34 to P-selectin is not dependent on sialylation but does require *O*-glycans and tyrosine sulfation.

Finally, we sought to validate the binding kinetics of CD34 in comparison with PSGL-1 using our SPR-based immunoprecipitation assay. The amount of detergent and salt was increased in this binding measurement relative to those in E-Ig in order to minimize the nonspecific interactions of P-Ig with the istoype control (see supplemental Materials and methods). As shown in Figure 7H, P-selectin binding to PSGL-1 and CD34 was Ca^{2+} dependent because binding was abolished when injected in the presence of EDTA. The mean K_D of P-Ig binding to PSGL-1 was 372 $\pm$ 5 nM, whereas that of P-Ig to CD34 was 621 $\pm$ 4 nM (Figure 7H). This difference is attributed to a difference in their dissociation rates, $k_{off\text{-}apparent}$ for CD34 $= 3 \times 10^{-4} \pm 0.1 \times 10^{-4}$ s^{-1} and for PSGL-1 $= 2 \times 10^{-4} \pm 0.3 \times 10^{-4}$ s^{-1}.

Discussion

For almost 30 years, the cell-surface sialomucin CD34 has been used as a marker to identify and enrich HSPCs in preparation for BM transplantation.[1] However, studies have revealed that the CD34^{neg} fraction of normal human BM is capable of differentiating into CD34^{pos} subsets that possess a more activated phenotype.[4-6,15] However, the CD34^{neg} fraction suffers from a profound impairment in migration after IV transplantation compared with the CD34^{pos} fraction.[5,7,8,11,13,49-52] Our flow cytometric and western blot data revealed a more pronounced E-selL activity on the CD34^{pos} subset of the Lin^{neg}CD38^{neg} fraction than on the CD34^{neg} subset, suggesting that the enhanced migratory ability of CD34^{pos} cells is due to its possession of a specific set of functional E-selLs, required for proper migration and homing of HSPCs. In agreement with these results, a previous study illustrated that BM and fetal liver–derived CD34^{pos} subsets rolled over immobilized E-selectin with higher efficiency than CD34^{neg} subsets.[53] Furthermore, microarray data analysis of CD34^{pos} vs CD34^{neg} subsets revealed exclusive expression of PSGL-1 and CD43 in the positive subset, suggesting that these ligands may be responsible for mediating interactions with E-selectin in this subset.[12] Note that the lack of the HCELL glycoform found here indicates that the higher expression of CD44 in the CD34^{neg} subset does not confer E-selectin binding

Figure 6. (continued) and subjected to western blotting for E-Ig (top panel) or CD34 (lower panel) as in panel B. (E) SPR analyses of OSGE treatment were performed as in panels A and C using 4H11-mAb (9000 RU) or its isotype control (6500 RU). (F) Western blot analysis of the treated CD34 immunoprecipitates were performed as in panels B and D. CD34 (Qbend-10) was used as an internal control to confirm *N*- and *O*-glycan removal. The sensorgrams presented are corrected for the bulk refractive index and nonspecific interactions using the isotype controls. All results are representative of n = 3 independent experiments.

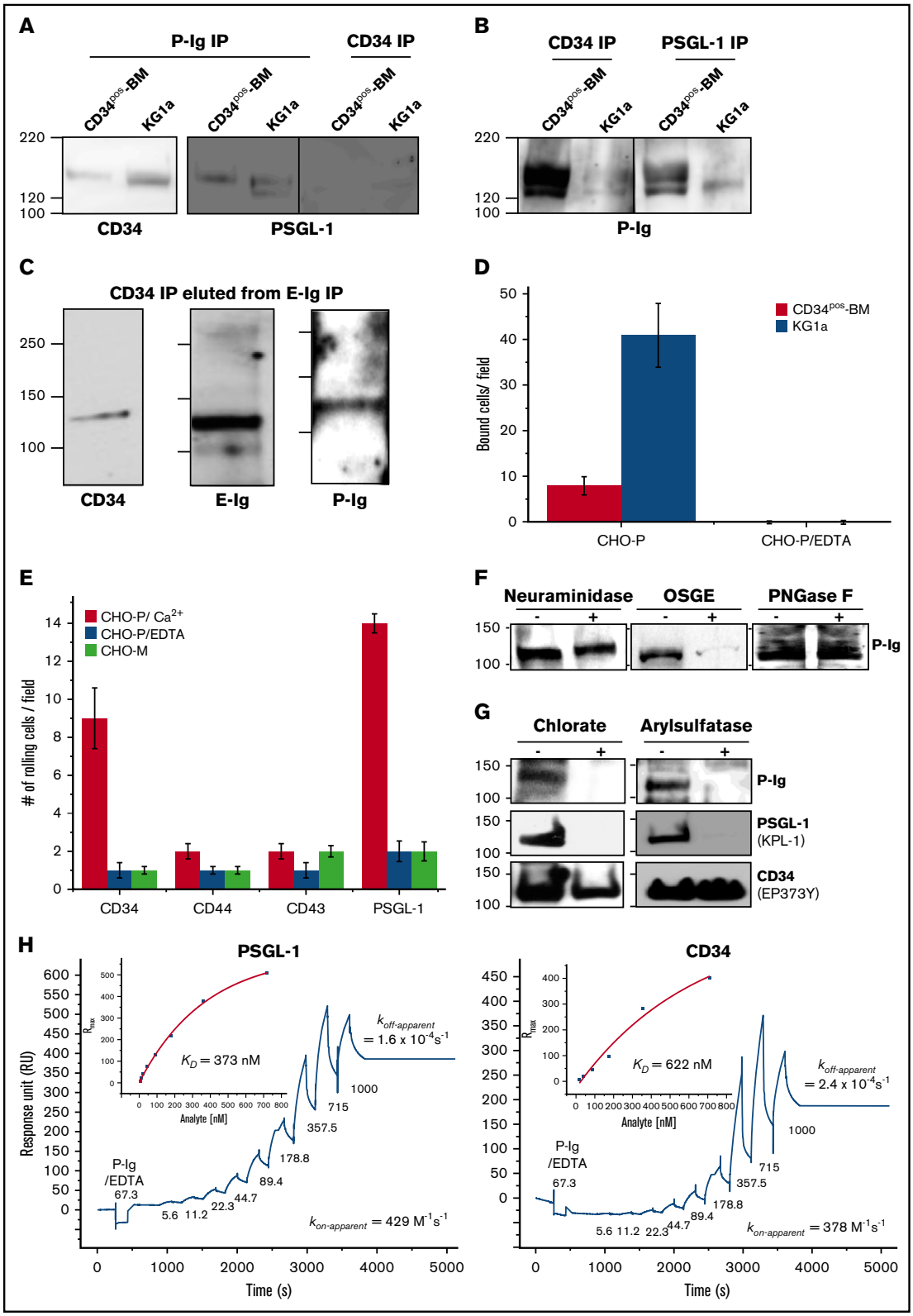

Figure 7. A novel CD34 glycoform acts as a P-selectin ligand and its interaction is dependent on *O*-glycans and tyrosine sulfation. (A) P-Ig was used to immunoprecipitate potential ligands from KG1a and CD34^{pos}-BM lysates, and the resultant proteins were analyzed by western blot for CD34 (QBend-10 and EP373Y mAb) or PSGL-1 (KPL-1-mAb). Note that CD34 immunoprecipitates were free from any PSGL-1 contamination (n = 3 independent experiments). (B) CD34 and PSGL-1 were immunoprecipitated from KG1a or CD34^{pos}-BM lysates and then analyzed by western blot for P-Ig binding (n = 3 independent experiments). (C) E-Ig was used to

activity, similar to that suggested previously.[32] A recent study also implied that distinct differences in other molecules critical to homing are also differentially expressed between these 2 populations of cells and may account for the inefficiencies in homing observed with CD34^{neg} subsets.[13] These results also elicit the question of whether the appropriate glycosyltransferases/glycosidases and/or appropriate substrates for these enzymes are differentially expressed in these subpopulations of HSPCs. Such an understanding of this valuable population of cells will allow researchers to harness technologies[34,54-57] that improve the migration capacity of these cells with the ultimate goal of using these cells in clinical settings.

Among several E-selL candidates suggested by our MS analysis, CD34 surfaced as an attractive ligand. CD34 is a heavily sialyated *O*-glycosylated type 1 transmembrane glycoprotein that is negatively charged and is speculated to behave in an antiadhesive manner, much like its relative mucin CD43.[19,58,59] Using a number of biochemical and functional assays, we provide evidence that CD34 from human HSPCs binds E-selectin similar to the other well-described E-selLs, CD44 (ie, HCELL) and PSGL-1. However, unlike CD34, CD43 has been shown to contribute only modestly to the E-selectin interaction.[34,60] Here, we document individual E-selL (CD34, CD44, and PSGL-1) binding affinities expressed on human HSPCs in their native form and show that all ligands display similar dissociation binding constants (K_D) with slow on- and off-rate kinetics consistent with previously reported data from our laboratory.[36,60] Blot-rolling assay results confirmed that CD43 has a weaker binding K_D by 1.8- to 2.0-fold because of the higher rate by which CD43 dissociates from E-Ig. Furthermore, using a CD34 knockdown approach, CD34 was found to play a crucial role in slowing down the velocity of rolling cells at shear stresses $\geq$3 dyne/cm^2. Interestingly, although an increase in E-Ig staining was observed in cell lysates from CD34 knockdown cells, this did not result in an increase in the number of rolling cells. This may be explained based on the TEM imaging data of KG1a cells outlined in this study. Knockdown of CD34 conclusively showed that microvilli structures were dramatically decreased on KG1a cells, implicating the importance of CD34 and CD34 family members in microvilli formation.[18,59,61,62] Interestingly, many studies suggest that microvilli protrusions are critical for mediating interactions between KG1a cells in flow and selectins (or endothelial cells). The microvilli undergo extensions and may form tethers,[63-69] so if these structures are eliminated by the knockdown of CD34, this would likely explain the effect on cell rolling. Furthermore, these data are in agreement with previous flow-based studies that showed that CD34 isolated from lysates of KG1a cells bound CHO-E cells[17] and that mouse thymocytes ectopically expressing CD34 specifically bound to human BM endothelial cells where control thymocytes not expressing CD34 did not.[10]

Both vascular selectins are required for human CD34^{pos} cell rolling and homing on BM microvessels, whereby defective rolling is only observed in E-/P-selectin double-knockout nonobese/severe combined immunodeficiency mice.[27] Indeed, P-selectin was found to significantly purify committed human HSPCs (CD34^{pos}CD38^{neg} cells) from total BM MNCs.[24,25,70] Our data show that CD34 on HSPCs can function as an alternative P-selectin ligand. Analysis of the glycan requirements of CD34 binding to P-selectin underscore similar characteristic modifications of PSGL-1 binding to P-selectin with 1 key difference[47,48]: both CD34 and PSGL-1 depend on *O*-glycosylation and tyrosine sulfation but only PSGL-1 requires sialylation to mediate binding.[71] However, the specific glycosylation profile needed for P-selectin recognition remains unknown. For example, P-selectin may bind to sialylated and nonsialylated forms of Le$^{x/a}$ structures.[72] Also, binding of TIM-1 (T-cell immunoglobulin and mucin domain 1), a major P-selectin ligand that controls the rolling of activated T cells, requires α1-3 fucosylation and tyrosine sulfation for efficient binding but not sialylation.[73] On a similar note, CD24, a sialoglycoprotein highly expressed in neutrophils as well as at early stages of B-cell development, does not display the sLe^x epitope but does carry a HNK-1 sulfate-containing epitope and the *O*-glycans that are required for such binding.[73-75] In addition to the modifications for P-selectin binding discussed above, CD34 also stained positive for the HNK-1 epitope, suggesting that it may also be important in mediating the binding of CD34 to P-selectin

Figure 7. (continued) immunoprecipitate E-selLs from the KG1a lysate and resultant proteins were eluted with 30 mM EDTA. The eluate was then immunoprecipitated with CD34 mAbs (clones 4H11 and 581) prior to western blot analysis for CD34, E-Ig, and P-Ig (n = 3 independent experiments). (D) CD34 immunoprecipitates were prepared from CD34^{pos}-BM and KG1a lysates and spotted on glass slides to test for CHO-P binding using a Stamper-Woodruff assay. Adherent CHO-P cells were counted by light microscopy. The data are a representative experiment, and the error bars indicate the SEM of 7 fields per slide on 2 slides for each experiment (n = 3 independent experiments). (E) Adhesion bar graph representing results obtained for the blot-rolling assay using CHO-P cell rolling (red bars) at 0.25 dyne/cm^2 (rolling cells per field) over western blots of immunoprecipitated CD34, CD44, CD43, or PSGL-1 from KG1a cell lysates as in Figure 3D. As controls, CHO-E cells were incubated with EDTA (blue bars) or mock-transfected CHO cells (CHO-M; light green bars) were used. The adhesion bar graph is the average of 4 fields of view per experiment from n = 5 independent experiments, and data are reported as the mean ± SEM (error bars). (F) CD34 immunoprecipitates from KG1a lysates were treated with neuraminidase, OSGE, or PNGase F or no treatment followed by western blot for P-Ig binding. Note that CD34 (QBend-10) was used as an internal control (data not shown) as in Figure 6 (n = 3 independent experiments). (G) To inhibit sulfation, KG1a cells were treated with 150 mM sodium chlorate for 72 hours (+; left panel) while KG1a whole-cell lysates were treated with 5 U/mL arylsulfatase for 3 hours (+; right panel) as described in supplemental Materials and methods. Negative controls consisted of the buffers used for the treatment without the sodium chlorate (−; left panel) while KG1a whole-cell lysates were treated arylsulfatase (−; right panel). Following treatment, CD34 was immunoprecipitated from cell lysates, and the resulting proteins were analyzed by western blot for P-Ig binding (top). Note that both treatments abrogated PSGL-1 binding to the KPL-1-mAb from KG1a lysates (middle; KPL-1 is sensitive to the loss of sulfation on PSGL-1), whereas the treatments did not significantly affect CD34 protein levels as indicated by EP373Y-mAb staining (bottom) or PSGL-1 staining (data not shown). Blots are representative of n = 3 independent experiments. (H) Divalent metal ion dependency and binding of P-Ig to PSGL-1 and CD34 captured from KG1a cell lysate at 150 mM NaCl were measured by injecting P-Ig (67 nM) in the presence of 10 mM EDTA followed by consecutive injection of different concentrations of P-Ig (as indicated) in the presence of 2 mM $CaCl_2$. The experimental conditions are similar to those in Figure 4 with P-Ig injected for 170 seconds interrupted by a 60-second washing buffer step. KPL-1-mAb (11 000 RU) or MsIgG$_1$ isotype control (5000 RU) were immobilized to capture PSGL-1 (left panel). 563-mAb (6527 RU) or MsIgG$_1$ isotype control (5000 RU) were immobilized to capture CD34 (right panel) (n = 3). $k_{off\text{-}apparent}$ and K_D were determined as described in Figures 3B and 4, respectively. The sensorgrams presented are corrected for the bulk refractive index and nonspecific interactions using the isotype controls.

(data not shown). The dissociation binding constants measured here for dimeric PSGL-1 and CD34 were 372 ± 5 and 621 ± 4 nM, respectively, which are in accordance with previous studies that reported a K_D of 320 ± 20 nM (with a k_{off} = 1.4 ± 0.1 s^{-1} and k_{on} = 4.4 × 10^6 M^{-1} s^{-1}) for monomeric P-selectin binding to PSGL-1 (isolated from human neutrophils).[76] The injection of membrane-derived P-selectin, mainly composed of dimeric and oligomeric forms of P-selectin, resulted in slower on and off rates compared with monomeric P-selectin.[76] Our data therefore have a characteristically similar K_D but with a slow apparent dissociation rate constant ($k_{off\text{-}apparent}$ ~10 000-fold increase) and a slow apparent association rate constant ($k_{on\text{-}apparent}$ ~100-fold reduction). This difference in binding kinetics of monomeric and dimeric forms of P-selectin is supported by previous studies.[76,77]

Our results show that treatment of KG1a cells with E-selectin resulted in their aggregation (supplemental Figure 3), and CD34 appeared to cluster toward lipid rafts, as indicated by an enhanced CTB staining pattern and intensity following E-selectin treatment. A number of studies have suggested that, prior to activation, CD34 is homogeneously distributed over the entire cell surface of HSPCs. However, following activation of these cells (via fibronectin or ligation using anti-CD34 antibodies), CD34 redistributes to lipid rafts and in some cases is even polarized toward the uropod, suggesting a role in enhanced homotypic adhesion.[78-81] In fact, studies comparing full-length CD34, a truncated form of CD34 (where most of the cytoplasmic domain is removed), and a chimeric molecule where the cytoplasmic domain of CD34 is fused with the extracellular domain of a cytokine receptor that is not believed to have a role in adhesion, implicate the cytoplasmic domain in the mediation of signaling events causing increased adhesion.[4,79] This role of CD34 in homotypic cell adhesion is significantly abrogated through the tyrosine kinase inhibitor and integrin mAb blockers for LFA-1 and ICAM-1, suggesting a concomitant activation of the LFA-1/ICAM-1 pathway.[79] Thus, CD34 clustering following E-Ig treatment could enhance adhesion, downstream of selectin binding by activating LFA-1/ICAM-1 integrins and/or unmasking adhesiveness of integrins to one another or toward the endothelium.[19,79,82]

The $CD34^{pos}$ population in AML is of special interest because the leukemic stem cells likely reside in this population.[83-85] Our work also reveals that a HECA-452 nonreactive form of CD34 that does not bind E-selectin was uniquely expressed on AML cells ($CD34^{pos}$ AML cells and KG1a cells) but not on normal $CD34^{pos}$ cells and could be considered a novel marker for this disease. Future studies using this glycoform of the protein as a target for the generation of mAbs may help to identify and target leukemic stem cells in the treatment of leukemia.[86,87] CD34 marker expression in AML is reported to be associated with poor prognosis and apoptosis-resistance markers.[88-90] Interestingly, CD34 fractions derived from AML samples with higher percentages of CD34 cells are more resistant to apoptosis than those derived from samples with a low CD34 percentage. In addition, apoptosis-related proteins are found to be differentially expressed among these populations,[91] showing higher expression of antiapoptotic proteins such as Bcl-2 and Bcl-xL in $CD34^{pos}$ vs $CD34^{neg}$ subpopulations. It is appealing to consider that the special glycoform of CD34 identified in our work could be involved in mediating this anti-apoptotic behavior.

Despite CD34 being widely renowned as a marker on HSPCs, the data outlined here consider a likely function for CD34 in helping mediate the migration of HSPCs through the formation of microvilli structures and via direct interactions with vascular selectins.

Acknowledgments

The authors sincerely thank Samah Z. Gadhoum for her help and support throughout the project and Samir Hamdan for his time and fruitful discussions regarding the SPR analyses. The authors express their gratitude to Maryam Mih and Samar A. Rustum for their support in the management of the laboratory and also to Mohammad Imran Khan for his assistance with the confocal microscopy. Wei Xu at Imaging and Characterization core facility at King Abdullah University of Science and Technology (KAUST) was very helpful at providing analysis software and training on the confocal microscopes. The authors also thank Carolyn Unck from the KAUST Academic Writing Service for editing the manuscript. In addition, a special thanks to Aswini K. Panigrahi (MS assistance) and Alaguraj Dharmarajnadar (cell sorting on BD Influx) from the Bioscience Core Laboratory Facility at KAUST.

This research was supported by a KAUST Faculty Baseline Research Funding Program and by a Competitive Research Grant (CRG_R2_13_MERZ_KAUST_1) (J.S.M.).

Authorship

Contribution: D.B.A. designed, performed, and analyzed experiments and wrote the manuscript; F.A.A., A.S.A.-A., H.M.J.A., and A.F.A. designed, performed, and analyzed experiments; H.M.J.A., P.B., and R.S. designed, performed, and analyzed the TEM imaging experiments; C.J.C. performed and analyzed the MS experiment; and J.S.M. conceived, designed, and analyzed experiments and wrote the manuscript.

Conflict-of-interest disclosure: The authors declare no competing financial interests.

The current affiliation for D.B.A. is Schepens Eye Research Institute, Massachusetts Eye & Ear, and Department of Ophthalmology, Harvard Medical School, Boston, MA.

ORCID profiles: D.B.A., 0000-0002-0974-5362; F.A.A., 0000-0001-6403-374X; A.S.A.-A., 0000-0002-8970-3807; H.M.J.A., 0000-0003-2172-2494; A.F.A., 0000-0002-4529-3156; R.S., 0000-0001-6476-1886; J.S.M., 0000-0002-7276-2907.

Correspondence: Jasmeen S. Merzaban, Ibn Al Haytham Building, level 4, Office 4218, 4700 King Abdullah University of Science and Technology, Thuwal 23955-6900, Saudi Arabia; e-mail: jasmeen.merzaban@kaust.edu.sa.

REFERENCES

1. Berenson RJ, Andrews RG, Bensinger WI, et al. Antigen CD34+ marrow cells engraft lethally irradiated baboons. *J Clin Invest*. 1988;81(3):951-955.

2. Osawa M, Hanada K, Hamada H, Nakauchi H. Long-term lymphohematopoietic reconstitution by a single CD34-low/negative hematopoietic stem cell. *Science*. 1996;273(5272):242-245.

3. Goodell MA, Rosenzweig M, Kim H, et al. Dye efflux studies suggest that hematopoietic stem cells expressing low or undetectable levels of CD34 antigen exist in multiple species. *Nat Med*. 1997;3(12):1337-1345.

4. Götze KS, Schiemann M, Marz S, et al. CD133-enriched CD34(-) (CD33/CD38/CD71)(-) cord blood cells acquire CD34 prior to cell division and hematopoietic activity is exclusively associated with CD34 expression. *Exp Hematol*. 2007;35(9):1408-1414.

5. Dooley DC, Oppenlander BK, Xiao M. Analysis of primitive CD34- and CD34+ hematopoietic cells from adults: gain and loss of CD34 antigen by undifferentiated cells are closely linked to proliferative status in culture. *Stem Cells*. 2004;22(4):556-569.

6. Nakamura Y, Ando K, Chargui J, et al. Ex vivo generation of CD34(+) cells from CD34(-) hematopoietic cells. *Blood*. 1999;94(12):4053-4059.

7. Sato T, Laver JH, Ogawa M. Reversible expression of CD34 by murine hematopoietic stem cells. *Blood*. 1999;94(8):2548-2554.

8. Dao MA, Arevalo J, Nolta JA. Reversibility of CD34 expression on human hematopoietic stem cells that retain the capacity for secondary reconstitution. *Blood*. 2003;101(1):112-118.

9. Wang J, Kimura T, Asada R, et al. SCID-repopulating cell activity of human cord blood-derived CD34- cells assured by intra-bone marrow injection. *Blood*. 2003;101(8):2924-2931.

10. Healy L, May G, Gale K, Grosveld F, Greaves M, Enver T. The stem cell antigen CD34 functions as a regulator of hemopoietic cell adhesion. *Proc Natl Acad Sci USA*. 1995;92(26):12240-12244.

11. Nielsen JS, McNagny KM. Influence of host irradiation on long-term engraftment by CD34-deficient hematopoietic stem cells. *Blood*. 2007;110(3):1076-1077.

12. Manfredini R, Zini R, Salati S, et al. The kinetic status of hematopoietic stem cell subpopulations underlies a differential expression of genes involved in self-renewal, commitment, and engraftment. *Stem Cells*. 2005;23(4):496-506.

13. Abe T, Matsuoka Y, Nagao Y, Sonoda Y, Hanazono Y. CD34-negative hematopoietic stem cells show distinct expression profiles of homing molecules that limit engraftment in mice and sheep. *Int J Hematol*. 2017;106(5):631-637.

14. Han Y, Gong ZY, Takakura N. Murine hematopoietic stem cell dormancy controlled by induction of a novel short form of PSF1 by histone deacetylase inhibitors. *Exp Cell Res*. 2015;334(2):183-193.

15. Anjos-Afonso F, Bonnet D. Forgotten gems: human CD34(-) hematopoietic stem cells. *Cell Cycle*. 2014;13(4):503-504.

16. Baumheter S, Singer MS, Henzel W, et al. Binding of L-selectin to the vascular sialomucin CD34. *Science*. 1993;262(5132):436-438.

17. Puri KD, Finger EB, Gaudernack G, Springer TA. Sialomucin CD34 is the major L-selectin ligand in human tonsil high endothelial venules. *J Cell Biol*. 1995;131(1):261-270.

18. Nielsen JS, McNagny KM. Novel functions of the CD34 family. *J Cell Sci*. 2008;121(Pt 22):3683-3692.

19. Drew E, Merzaban JS, Seo W, Ziltener HJ, McNagny KM. CD34 and CD43 inhibit mast cell adhesion and are required for optimal mast cell reconstitution. *Immunity*. 2005;22(1):43-57.

20. Lehr JE, Pienta KJ. Preferential adhesion of prostate cancer cells to a human bone marrow endothelial cell line. *J Natl Cancer Inst*. 1998;90(2):118-123.

21. Schweitzer KM, Dräger AM, van der Valk P, et al. Constitutive expression of E-selectin and vascular cell adhesion molecule-1 on endothelial cells of hematopoietic tissues. *Am J Pathol*. 1996;148(1):165-175.

22. Schweitzer KM, Vicart P, Delouis C, et al. Characterization of a newly established human bone marrow endothelial cell line: distinct adhesive properties for hematopoietic progenitors compared with human umbilical vein endothelial cells. *Lab Invest*. 1997;76(1):25-36.

23. Sipkins DA, Wei X, Wu JW, et al. In vivo imaging of specialized bone marrow endothelial microdomains for tumour engraftment. *Nature*. 2005;435(7044):969-973.

24. Wojciechowski JC, Narasipura SD, Charles N, et al. Capture and enrichment of CD34-positive haematopoietic stem and progenitor cells from blood circulation using P-selectin in an implantable device. *Br J Haematol*. 2008;140(6):673-681.

25. Narasipura SD, Wojciechowski JC, Charles N, Liesveld JL, King MR. P-Selectin coated microtube for enrichment of CD34+ hematopoietic stem and progenitor cells from human bone marrow. *Clin Chem*. 2008;54(1):77-85.

26. Nabors LK, Wang LD, Wagers AJ, Kansas GS. Overlapping roles for endothelial selectins in murine hematopoietic stem/progenitor cell homing to bone marrow. *Exp Hematol*. 2013;41(7):588-596.

27. Hidalgo A, Weiss LA, Frenette PS. Functional selectin ligands mediating human CD34(+) cell interactions with bone marrow endothelium are enhanced postnatally. *J Clin Invest*. 2002;110(4):559-569.

28. Mazo IB, Gutierrez-Ramos JC, Frenette PS, Hynes RO, Wagner DD, von Andrian UH. Hematopoietic progenitor cell rolling in bone marrow microvessels: parallel contributions by endothelial selectins and vascular cell adhesion molecule 1 [published correction appears in *J Exp Med*. 1998;188(5):1001]. *J Exp Med*. 1998;188(3):465-474.

29. Frenette PS, Subbarao S, Mazo IB, von Andrian UH, Wagner DD. Endothelial selectins and vascular cell adhesion molecule-1 promote hematopoietic progenitor homing to bone marrow. *Proc Natl Acad Sci USA*. 1998;95(24):14423-14428.

30. Wiese G, Barthel SR, Dimitroff CJ. Analysis of physiologic E-selectin-mediated leukocyte rolling on microvascular endothelium. *J Vis Exp*. 2009;(24):e1009.

31. Hao QL, Shah AJ, Thiemann FT, Smogorzewska EM, Crooks GM. A functional comparison of CD34 + CD38- cells in cord blood and bone marrow. *Blood*. 1995;86(10):3745-3753.

32. Dimitroff CJ, Lee JY, Rafii S, Fuhlbrigge RC, Sackstein R. CD44 is a major E-selectin ligand on human hematopoietic progenitor cells. *J Cell Biol*. 2001;153(6):1277-1286.

33. Katayama Y, Hidalgo A, Furie BC, Vestweber D, Furie B, Frenette PS. PSGL-1 participates in E-selectin-mediated progenitor homing to bone marrow: evidence for cooperation between E-selectin ligands and alpha4 integrin. *Blood*. 2003;102(6):2060-2067.

34. Merzaban JS, Burdick MM, Gadhoum SZ, et al. Analysis of glycoprotein E-selectin ligands on human and mouse marrow cells enriched for hematopoietic stem/progenitor cells. *Blood*. 2011;118(7):1774-1783.

35. Sackstein R. Fulfilling Koch's postulates in glycoscience: HCELL, GPS and translational glycobiology. *Glycobiology*. 2016;26(6):560-570.

36. AbuSamra DB, Al-Kilani A, Hamdan SM, Sakashita K, Gadhoum SZ, Merzaban JS. Quantitative characterization of E-selectin interaction with native CD44 and P-selectin glycoprotein ligand-1 (PSGL-1) using a real time immunoprecipitation-based binding assay. *J Biol Chem*. 2015;290(35): 21213-21230.

37. Stamper HB Jr, Woodruff JJ. Lymphocyte homing into lymph nodes: in vitro demonstration of the selective affinity of recirculating lymphocytes for high-endothelial venules. *J Exp Med*. 1976;144(3):828-833.

38. Fuhlbrigge RC, King SL, Dimitroff CJ, Kupper TS, Sackstein R. Direct real-time observation of E- and P-selectin-mediated rolling on cutaneous lymphocyte-associated antigen immobilized on Western blots. *J Immunol*. 2002;168(11):5645-5651.

39. Sackstein R, Fuhlbrigge R. Western blot analysis of adhesive interactions under fluid shear conditions: the blot rolling assay. *Methods Mol Biol*. 2009; 536:343-354.

40. Hernandez Mir G, Helin J, Skarp KP, et al. Glycoforms of human endothelial CD34 that bind L-selectin carry sulfated sialyl Lewis x capped O- and N-glycans. *Blood*. 2009;114(3):733-741.

41. Lanza F, Healy L, Sutherland DR. Structural and functional features of the CD34 antigen: an update. *J Biol Regul Homeost Agents*. 2001;15(1):1-13.

42. Martinez M, Joffraud M, Giraud S, et al. Regulation of PSGL-1 interactions with L-selectin, P-selectin, and E-selectin: role of human fucosyltransferase-IV and -VII. *J Biol Chem*. 2005;280(7):5378-5390.

43. Lévesque JP, Zannettino AC, Pudney M, et al. PSGL-1-mediated adhesion of human hematopoietic progenitors to P-selectin results in suppression of hematopoiesis. *Immunity*. 1999;11(3):369-378.

44. Spertini O, Cordey AS, Monai N, Giuffrè L, Schapira M. P-selectin glycoprotein ligand 1 is a ligand for L-selectin on neutrophils, monocytes, and CD34+ hematopoietic progenitor cells. *J Cell Biol*. 1996;135(2):523-531.

45. Mintz KP, Fisher LW, Grzesik WJ, Hascall VC, Midura RJ. Chlorate-induced inhibition of tyrosine sulfation on bone sialoprotein synthesized by a rat osteoblast-like cell line (UMR 106-01 BSP). *J Biol Chem*. 1994;269(7):4845-4852.

46. Snapp KR, Ding H, Atkins K, Warnke R, Luscinskas FW, Kansas GS. A novel P-selectin glycoprotein ligand-1 monoclonal antibody recognizes an epitope within the tyrosine sulfate motif of human PSGL-1 and blocks recognition of both P- and L-selectin. *Blood*. 1998;91(1):154-164.

47. Wilkins PP, Moore KL, McEver RP, Cummings RD. Tyrosine sulfation of P-selectin glycoprotein ligand-1 is required for high affinity binding to P-selectin. *J Biol Chem*. 1995;270(39):22677-22680.

48. Sako D, Comess KM, Barone KM, Camphausen RT, Cumming DA, Shaw GD. A sulfated peptide segment at the amino terminus of PSGL-1 is critical for P-selectin binding. *Cell*. 1995;83(2):323-331.

49. Sonoda Y. Immunophenotype and functional characteristics of human primitive CD34-negative hematopoietic stem cells: the significance of the intra-bone marrow injection. *J Autoimmun*. 2008;30(3):136-144.

50. Lemoli RM, Bertolini F, Petrucci MT, et al. Functional and kinetic characterization of granulocyte colony-stimulating factor-primed CD34- human stem cells [published correction appears in *Br J Haematol*. 2004;124(2):256]. *Br J Haematol*. 2003;123(4):720-729.

51. Gao Z, Fackler MJ, Leung W, et al. Human CD34+ cell preparations contain over 100-fold greater NOD/SCID mouse engrafting capacity than do CD34-cell preparations. *Exp Hematol*. 2001;29(7):910-921.

52. Verfaillie CM, Almeida-Porada G, Wissink S, Zanjani ED. Kinetics of engraftment of CD34(-) and CD34(+) cells from mobilized blood differs from that of CD34(-) and CD34(+) cells from bone marrow. *Exp Hematol*. 2000;28(9):1071-1079.

53. Greenberg AW, Kerr WG, Hammer DA. Relationship between selectin-mediated rolling of hematopoietic stem and progenitor cells and progression in hematopoietic development. *Blood*. 2000;95(2):478-486.

54. Merzaban JS, Imitola J, Starossom SC, et al. Cell surface glycan engineering of neural stem cells augments neurotropism and improves recovery in a murine model of multiple sclerosis. *Glycobiology*. 2015;25(12):1392-1409.

55. Sackstein R, Merzaban JS, Cain DW, et al. Ex vivo glycan engineering of CD44 programs human multipotent mesenchymal stromal cell trafficking to bone. *Nat Med*. 2008;14(2):181-187.

56. Broxmeyer HE, Capitano M, Campbell TB, Hangoc G, Cooper S. Modulation of Hematopoietic Chemokine Effects In Vitro and In Vivo by DPP-4/CD26. *Stem Cells Dev*. 2016;25(8):575-585.

57. Christopherson KW II, Hangoc G, Mantel CR, Broxmeyer HE. Modulation of hematopoietic stem cell homing and engraftment by CD26. *Science*. 2004; 305(5686):1000-1003.

58. Ardman B, Sikorski MA, Staunton DE. CD43 interferes with T-lymphocyte adhesion. *Proc Natl Acad Sci USA*. 1992;89(11):5001-5005.

59. Ohnishi H, Sasaki H, Nakamura Y, et al. Regulation of cell shape and adhesion by CD34. *Cell Adhes Migr*. 2013;7(5):426-433.

60. Ali AJ, Abuelela AF, Merzaban JS. An analysis of trafficking receptors shows that CD44 and P-selectin glycoprotein ligand-1 collectively control the migration of activated human T-cells. *Front Immunol*. 2017;8:492.

61. Furness SG, McNagny K. Beyond mere markers: functions for CD34 family of sialomucins in hematopoiesis. *Immunol Res*. 2006;34(1):13-32.

62. Nielsen JS, Graves ML, Chelliah S, Vogl AW, Roskelley CD, McNagny KM. The CD34-related molecule podocalyxin is a potent inducer of microvillus formation. *PLoS One*. 2007;2(2):e237.

63. Park EY, Smith MJ, Stropp ES, et al. Comparison of PSGL-1 microbead and neutrophil rolling: microvillus elongation stabilizes P-selectin bond clusters. *Biophys J*. 2002;82(4):1835-1847.

64. Ramachandran V, Williams M, Yago T, Schmidtke DW, McEver RP. Dynamic alterations of membrane tethers stabilize leukocyte rolling on P-selectin. *Proc Natl Acad Sci USA*. 2004;101(37):13519-13524.

65. Schmidtke DW, Diamond SL. Direct observation of membrane tethers formed during neutrophil attachment to platelets or P-selectin under physiological flow. *J Cell Biol*. 2000;149(3):719-730.

66. Sundd P, Gutierrez E, Pospieszalska MK, Zhang H, Groisman A, Ley K. Quantitative dynamic footprinting microscopy reveals mechanisms of neutrophil rolling. *Nat Methods*. 2010;7(10):821-824.

67. Sundd P, Gutierrez E, Koltsova EK, et al. 'Slings' enable neutrophil rolling at high shear. *Nature*. 2012;488(7411):399-403.

68. Sundd P, Pospieszalska MK, Ley K. Neutrophil rolling at high shear: flattening, catch bond behavior, tethers and slings. *Mol Immunol*. 2013;55(1):59-69.

69. Marki A, Buscher K, Mikulski Z, Pries A, Ley K. Rolling neutrophils form tethers and slings under physiologic conditions in vivo [published online ahead of print 18 August 2017]. *J Leukoc Biol*. 2017. doi:10.1189/jlb.1AB0617-230R.

70. Zannettino AC, Berndt MC, Butcher C, Butcher EC, Vadas MA, Simmons PJ. Primitive human hematopoietic progenitors adhere to P-selectin (CD62P). *Blood*. 1995;85(12):3466-3477.

71. Moore KL, Stults NL, Diaz S, et al. Identification of a specific glycoprotein ligand for P-selectin (CD62) on myeloid cells. *J Cell Biol*. 1992;118(2):445-456.

72. Nelson RM, Dolich S, Aruffo A, Cecconi O, Bevilacqua MP. Higher-affinity oligosaccharide ligands for E-selectin. *J Clin Invest*. 1993;91(3):1157-1166.

73. Angiari S, Donnarumma T, Rossi B, et al. TIM-1 glycoprotein binds the adhesion receptor P-selectin and mediates T cell trafficking during inflammation and autoimmunity. *Immunity*. 2014;40(4):542-553.

74. Pirruccello SJ, LeBien TW. The human B cell-associated antigen CD24 is a single chain sialoglycoprotein. *J Immunol*. 1986;136(10):3779-3784.

75. Aigner S, Sthoeger ZM, Fogel M, et al. CD24, a mucin-type glycoprotein, is a ligand for P-selectin on human tumor cells. *Blood*. 1997;89(9):3385-3395.

76. Mehta P, Cummings RD, McEver RP. Affinity and kinetic analysis of P-selectin binding to P-selectin glycoprotein ligand-1. *J Biol Chem*. 1998;273(49):32506-32513.

77. Molenaar TJ, Appeldoorn CC, de Haas SA, et al. Specific inhibition of P-selectin-mediated cell adhesion by phage display-derived peptide antagonists. *Blood*. 2002;100(10):3570-3577.

78. Wagner W, Saffrich R, Wirkner U, et al. Hematopoietic progenitor cells and cellular microenvironment: behavioral and molecular changes upon interaction. *Stem Cells*. 2005;23(8):1180-1191.

79. Hu MC, Chien SL. The cytoplasmic domain of stem cell antigen CD34 is essential for cytoadhesion signaling but not sufficient for proliferation signaling. *Blood*. 1998;91(4):1152-1162.

80. Altrock E, Muth CA, Klein G, Spatz JP, Lee-Thedieck C. The significance of integrin ligand nanopatterning on lipid raft clustering in hematopoietic stem cells. *Biomaterials*. 2012;33(11):3107-3118.

81. Giebel B, Corbeil D, Beckmann J, et al. Segregation of lipid raft markers including CD133 in polarized human hematopoietic stem and progenitor cells. *Blood*. 2004;104(8):2332-2338.

82. Majdic O, Stöckl J, Pickl WF, et al. Signaling and induction of enhanced cytoadhesiveness via the hematopoietic progenitor cell surface molecule CD34. *Blood*. 1994;83(5):1226-1234.

83. Lapidot T, Sirard C, Vormoor J, et al. A cell initiating human acute myeloid leukaemia after transplantation into SCID mice. *Nature*. 1994;367(6464):645-648.

84. Bonnet D, Dick JE. Human acute myeloid leukemia is organized as a hierarchy that originates from a primitive hematopoietic cell. *Nat Med*. 1997;3(7):730-737.

85. Zeijlemaker W, Kelder A, Oussoren-Brockhoff YJ, et al. A simple one-tube assay for immunophenotypical quantification of leukemic stem cells in acute myeloid leukemia. *Leukemia*. 2016;30(2):439-446.

86. Pollyea DA, Jordan CT. Therapeutic targeting of acute myeloid leukemia stem cells. *Blood*. 2017;129(12):1627-1635.

87. Gadhoum SZ, Madhoun NY, Abuelela AF, Merzaban JS. Anti-CD44 antibodies inhibit both mTORC1 and mTORC2: a new rationale supporting CD44-induced AML differentiation therapy. *Leukemia*. 2016;30(12):2397-2401.

88. Pallis M, Russell N. P-glycoprotein plays a drug-efflux-independent role in augmenting cell survival in acute myeloblastic leukemia and is associated with modulation of a sphingomyelin-ceramide apoptotic pathway. *Blood*. 2000;95(9):2897-2904.

89. Wuchter C, Karawajew L, Ruppert V, et al. Clinical significance of CD95, Bcl-2 and Bax expression and CD95 function in adult de novo acute myeloid leukemia in context of P-glycoprotein function, maturation stage, and cytogenetics. *Leukemia*. 1999;13(12):1943-1953.

90. Zhang Y, Zhou SY, Yan HZ, et al. miR-203 inhibits proliferation and self-renewal of leukemia stem cells by targeting survivin and Bmi-1. *Sci Rep*. 2016;6:19995.

91. van Stijn A, van der Pol MA, Kok A, et al. Differences between the CD34+ and CD34- blast compartments in apoptosis resistance in acute myeloid leukemia. *Haematologica*. 2003;88(5):497-508.